HHS Public Access

Author manuscript

*Neuroimage*. Author manuscript; available in PMC 2021 September 01.

Published in final edited form as:

*Neuroimage*. 2021 August 01; 236: 118026. doi:10.1016/j.neuroimage.2021.118026.

# Longitudinal fMRI measures of cortical reactivation and hand use with and without training after sensory loss in primates

**Hui-Xin Qi**[a,1,*], **Jamie L. Reed**[a,1], **Feng Wang**[b,c], **Christopher L. Gross**[a], **Xin Liu**[a,2], **Li Min Chen**[b,c], **Jon H. Kaas**[a,b]

[a]Department of Psychology, Vanderbilt University, Nashville, TN 37240, USA

[b]Institute of Imaging Science, Vanderbilt University, Nashville, TN 37240, USA

[c]Radiology and Radiological Sciences, Vanderbilt University, Nashville, TN 37240, USA

## Abstract

In a series of previous studies, we demonstrated that damage to the dorsal column in the cervical spinal cord deactivates the contralateral somatosensory hand cortex and impairs hand use in a reach-to-grasp task in squirrel monkeys. Nevertheless, considerable cortical reactivation and behavioral recovery occurs over the following weeks to months after lesion. This timeframe may also be a window for targeted therapies to promote cortical reactivation and functional reorganization, aiding in the recovery process. Here we asked if and how task specific training of an impaired hand would improve behavioral recovery and cortical reorganization in predictable ways, and if recovery related cortical changes would be detectable using noninvasive functional magnetic resonance imaging (fMRI). We further asked if invasive neurophysiological mapping reflected fMRI results. A reach-to-grasp task was used to test impairment and recovery of hand use before and after dorsal column lesions (DC-lesion). The activation and organization of the affected primary somatosensory cortex (area 3b) was evaluated with two types of fMRI – either blood oxygenation level dependent (BOLD) or cerebral blood volume (CBV) with a contrast agent of monocrystalline iron oxide nanocolloid (MION) – before and after DC-lesion. At the end of the behavioral and fMRI studies, microelectrode recordings in the somatosensory areas 3a, 3b and 1 were used to characterize neuronal responses and verify the somatotopy of cortical reactivations. Our results indicate that even after nearly complete DC lesions, monkeys had both considerable post-lesion behavioral recovery, as well as cortical reactivation assessed with fMRI followed by extracellular recordings. Generalized linear regression analyses indicate that



[*]Correspondence author. huixin.qi@vanderbilt.edu (H.-X. Qi).

[1]Co-first authors

[2]Present address: University Counseling Service, Beijing International Studies University, Beijing, 100024, China

Author contributions

**Hui-Xin Qi**: Investigation, Data curation, Formal analysis, Writing – Original draft & Editing. **Jamie L. Reed**: Data curation, Formal analysis, Writing-Reviewing and Editing. **Feng Wang**: Data curation, Software, Writing-Reviewing and Editing. **Christopher L. Gross**: Formal analysis, Writing – Review & Editing. **Xin Liu**: Formal analysis. **Li Min Chen**: Conceptualization, Methodology for fMRI data collection and interpretation. **Jon H. Kaas**: Supervision, Writing – Review & Editing.

Declarations of Competing Interest

None.

Supplementary materials

Supplementary material associated with this article can be found, in the online version, at doi:10.1016/j.neuroimage.2021.118026.

lesion extent is correlated with the behavioral outcome, as well as with the difference in the percent signal change from pre-lesion peak activation in fMRI. Monkeys showed behavioral recovery and nearly complete cortical reactivation by 9–12 weeks post-lesion (particularly when the DC-lesion was incomplete). Importantly, the specific training group revealed trends for earlier behavioral recovery and had higher magnitude of fMRI responses to digit stimulation by 5–8 weeks post-lesion. Specific kinematic measures of hand movements in the selected retrieval task predicted recovery time and related to lesion characteristics better than overall task performance success. For measures of cortical reactivation, we found that CBV scans provided stronger signals to vibrotactile digit stimulation as compared to BOLD scans, and thereby may be the preferred non-invasive way to study the cortical reactivation process after sensory deprivations from digits. When the reactivation of cortex for each of the digits was considered, the reactivation by digit 2 stimulation as measured with microelectrode maps and fMRI maps was best correlated with overall behavioral recovery.

**Keywords**

Primates; Somatosensory cortex; Spinal cord injury; Plasticity; Rehabilitation

## 1. Introduction

Little is known about how parameters of intensive behavioral therapy influence the reorganization of processing systems in the brain and behavioral recovery. Here we applied a food retrieval task in an established model of incomplete spinal cord injury that affects sensation of one hand in squirrel monkeys, and we sought to examine whether longitudinal imaging and behavioral measures distinguished between cases with rehabilitation-like training. We further investigated the relationship between the noninvasive measures of brain activity and behavior with invasive measures of neuronal activity in cortex and histological measures of spinal cord injury.

In a series of previous studies, we demonstrated that a high, but incomplete cervical lesion of the dorsal columns in monkeys immediately deactivated the contralateral hand representation in the primary somatosensory cortex (area 3b) and higher somatosensory representations areas 1, S2, PV (Jain et al., 1997, 2008; Qi et al., 2011; Chen et al., 2012; Yang et al., 2014; Qi et al., 2019). The sense of touch on the affected hand was greatly impaired, as evidenced by difficulties in a food pellet retrieval task and a reluctance to use the affected hand in reaching for food, but locomotor behavior appeared to be normal (Qi et al., 2013). Remarkably, over weeks to months of recovery, the activation of the affected somatosensory cortex by inputs from the hand and dexterity of hand use returned. Similar results were obtained in monkeys after incomplete deafferentations of hand by sectioning some of the cervical dorsal roots unilaterally (Darian–Smith and Ciferri, 2005; Fisher et al., 2020; see Darian–Smith and Fisher, 2019 for review). As reactivation of hand cortex returned, hand use in retrieving small pellets of food as in other tasks improved. Thus, reactivation of hand cortex by hand inputs appears to have important functional consequences.

To more accurately measure the extent of dorsal column lesions, we quantified the effectiveness of the spinal cord lesions by using tracers to label the terminals of surviving afferents from digits of the affected hand in the cuneate nucleus (Qi et al., 2011). By comparing the magnitude of these surviving afferents to matching inputs from digits of the intact hand to the cuneate nuclei, we were able to estimate the percent loss of DC afferents from the hand. This method allowed us to relate the proportional loss of DC afferents to the cuneate nuclei to the extent and somatotopy of the cortical reactivation in area 3b, and to behavioral recovery (Qi et al., 2011). In addition, our understanding of the relationship of lesion completeness to cortical reactivation and behavioral recovery led us to consider intensive task-specific therapy as an avenue for improving the quality of behavioral recoveries.

In an earlier study from our group, sensory intensive behavioral training was found to result in a more normal somatotopy and neuronal receptive field sizes in somatosensory cortex after section and repair of the median nerve of hand in early postnatal life of macaque monkeys (Florence et al., 2001). The study found that a significantly higher proportion of neurons in the somatosensory cortical area 3b had both small and somatotopically appropriate receptive fields when compared to those of non-trained, nerve injured control monkeys. These data suggested that “such repetitive training would facilitate use-dependent mechanisms of synaptic selection, which are already known to have a powerful influence on somatosensory cortical organization” (Merzenich et al., 1996). Here we further asked if intensive behavioral therapy of the impaired hand has an impact on behavioral recovery and cortical reorganization after a DC-lesion. Evidence of even a modest improvement in behavioral recovery as a result of therapy would warrant evaluation of more intensive behavioral approaches. Previously, behavioral training in hand use has demonstrated effectiveness in improving recoveries after partial lesions of the hand representation in motor cortex in both monkeys (e.g., Nudo et al., 1996a, b; see Nudo, 2013 for review) and humans (Taub et al, 2002, 2014). Intensive behavioral therapy is the most widely used and effective treatment for promoting functional recovery after stroke or spinal cord injury (Krajacic et al., 2010; Andrews et al., 2020; see Dietz and Fouad, 2014; Dietz, 2016; Burns et al., 2017; Edwards et al., 2019 for review).

In order to determine if task specific therapy of the impaired hand improves either the behavioral recovery, cortical reorganization, or both, a “reach-to-grasp” task was used to evaluate degree of impairment and recovery of the affected hand both before and after DC-lesion. The activation and organization of the affected somatosensory cortex (area 3b) was evaluated longitudinally before and after the DC-lesion with two types of fMRI, either blood oxygenation level dependent (BOLD) or cerebral blood volume (CBV). Then, at the end of the behavioral and fMRI studies, the neuronal response properties in the reactivated regions of area 3b (in the same group of monkeys) were characterized from electrophysiological recordings with either a single microelectrode or with 100-electrode arrays. This overall approach allowed us to determine the spatiotemporal trajectory of recoveries in a more precise way than before. Although fMRI has been widely used to reveal cortical activation in patients with peripheral and central nervous system injuries, fMRI has limited spatiotemporal resolution. To overcome this limitation, we used fMRI to first reveal when and where functional recoveries took place, then used microelectrodes or

microelectrode arrays to obtain high resolution maps of the reactivated cortex under the guidance of the fMRI activation map. In addition, the neuronal response properties were characterized in the reactivated regions of cortex that had been identified via fMRI. Thus, we were able to directly relate the physiological results to the behavioral results and the completeness of the loss of direct sensory inputs to the cuneate nucleus.

Our results indicate that even when the DC-lesion was extensive, monkeys showed considerable post-lesion behavioral recovery and cortical reactivation. Intensive therapy with the impaired hand tended to promote earlier behavioral recovery and earlier cortical reactivation. Reactivation of cortical territories in area 3b by inputs from both digits 1 and 2 best correlated with behavior recoveries.

## 2. Materials and methods

Nine adult male New World squirrel monkeys (4 *Saimiri sciureus, 3 Saimiri boliviensis, 2 Saimiri peruvian boliviensis*) were used in this study. Subjects were three to five years old and weighed 800–1200 g. All experimental procedures were approved by the Vanderbilt University Animal Care and Use Committee, and followed the guidelines of the National Institute of Health Guides for the Care and Use of Laboratory Animals. Related results from some of these monkeys have been published previously (Liao et al., 2016; Qi et al., 2019).

### 2.1. Experimental design

As shown in Fig. 1A, prior to surgery, monkeys were trained and tested on a “reach-to-grasp” task aimed at evaluating post-lesion impairment of hand use and training effects. In addition, the somatotopy of the hand representation in cortical area 3b was determined with functional magnetic resonance imaging (fMRI) before, and several times after the unilateral dorsal columns lesion (DC-lesion) in the cervical spinal cord. Next, monkeys were tested post DC-lesion on the reach-to-grasp task for up to 1 week before the terminal procedures. For the intensive therapy group, monkeys were trained in the same task 30–60 min per day, five days per week for up to three months. Four to six days before the terminal procedure, distal phalanges of digits 1, 3, and 5 (D1, D3, and D5) of both hands were injected with transganglionic tracer to label spared afferents in the dorsal column and axon terminals in the cuneate nuclei. The effectiveness of the lesion in disrupting sensory input was assessed by comparing labeling patterns of the intact side to those of the lesion side. In a terminal procedure, the responsiveness and somatotopies of the hand representations in cortical area 3b were characterized using multi-unit recordings with a single electrode or a microelectrode array. At the end of the recording session, each monkey was injected with a lethal dose of anesthetic and subsequently perfused with a fixative (see Tissue processing), after which the brains and spinal cords were extracted for processing.

### 2.2. Behavioral training and testing

A reach-to-grasp task was used to determine the degree of impairment and subsequent recovery of hand use after the DC-lesion (detailed methods are described in Qi et al., 2013). In brief, nine freely moving monkeys were preoperatively trained for two to four weeks to grasp and retrieve 45 mg sugar pellets from a modified Kluver Board mounted in front

of their home cage. The testing board contained four wells of incrementally increasing difficulty, where well 1 (W1) was the easiest (shallow) and well 4 (W4) was most difficult (deep). The diameter of deeper wells 3 and 4 was 1.14 cm, in which the well sizes could fit a maximum of 2 fingers of the squirrel monkey. Typically, the monkey initially contacted the food pellet inside of the wells and subsequently pulled out the pellet with digit 2 alone or digits 2 and 3, and secured it against D1 and palm. The thumb was typically flexed throughout the grasp and was therefore not directly involved in handling the food pellet, but helped to secure the pellet during retrieval. Thus, grasping in the present task was achieved with a power grip (Fig. 1B). The performance was video recorded for scoring and trajectory analysis. Five monkeys (SM-Fr, SM-Fy, SM-Kr, SM-Ur, SM-Ya; Table 1) received post-operative intensive therapy of the impaired hand in the reach-to-grasp task five days a week, with up to 200 retrieval trials per training day over a period of three months. The intensive therapy tended to begin with the easy well (W1) around the fifth day post-lesion, however, the actual starting day of data collection depended on the monkey's capability after DC-lesion. Each therapy session usually lasted up to one hour. The difficulty of the reach-to-grasp task was gradually increased until the monkey was able to retrieve pellets from the most difficult well (W4), and the training was retained on W4 thereafter. Seven out of nine monkeys were tested one or two times a week in the same reach-to-grasp task, resulting in about 100 retrievals per testing week. The other two monkeys (SM-Bu and SM-Hn) were tested with fewer trials with other small food items each week on the same task due to refusal to accept sugar pellets. Overall, four monkeys in the minimum behavioral therapy group performed less than 200 trials per week on easy and difficult wells, while five monkeys in the intensive therapy group performed about 1000 trials per week on difficult wells.

The behavior analysis was scored by trained raters who were blinded to the animal's therapy condition. The two main categories used for scoring were: (1) Percent of success and number of digit flexes (attempts) per successful trial and, (2) Kinematic analysis of hand movement trajectory during successful retrieval. Each trial of hand trajectory was divided into three segments: reach, grasp, and retrieval. (A) *Reach* was considered when the forelimb was transported from inside the home cage, through the aperture, and the hand was pronated onto the board. (B) *Grasp* was considered when the digits were flexed to contact the food pellet, and the pellet was typically secured between digits 1, 2, and 3 (D1, D2, and D3). (C) *Retrieval* was considered when the wrist was supinated as the forelimb was withdrawn from the board and into the cage. The amount of time to execute each segment (reach, grasp, and retrieval) and its spatial trajectory were measured from the video records. Since D2 was visible throughout the video records for all three segments, we used the joint between the proximal and middle phalanges as the tracking point. The kinematic analysis was limited to the first five successful trials in the easiest well (W1), and tracking was done frame-by-frame using Quick Time software (see Qi et al., 2013 for detail). In order to quantify the kinematics of hand movement during the task, we measured the amount of time and spatial trajectory (Distance) for each segment (reach, grasp, retrieval) frame-by-frame from the video records, then calculated speeds from these two parameters. A transparency was mounted onto a computer screen and position of the tracking point was marked with a color-coded dot for each video frame. The dots that comprised each segment were serially

connected with straight lines. The length of each connecting line was measured with a compass. The sum of measurements was calculated for each segment to determine the Distances of reach, grasp, and retrieval, and the number of video frames (33 ms/frame) was used to determine the Time of each segment. Due to slight variations in camera position used across filming days, the Distance was calibrated based on the known width of the cage aperture (Qi et al., 2013).

### 2.3. FMRI data acquisition

Monkeys were scanned in a 9.4T 21-cm narrow-bore Agilent MRI magnet using a 3 cm surface transmit-receive coil secured over primary somatosensory area 3b. For details, see Chen et al., 2012, Qi and Wang et al., 2016a. Each monkey was anesthetized with isoflurane (0.5–1.1%) delivered by a mixture of $N_2O/O_2$ in a 70:30 ratio and mechanically ventilated during MRI scans. During fMRI data acquisition, isoflurane level was typically maintained between 0.8–1%. The head and body were stabilized in an MRI compatible frame. Vital signs were monitored and maintained throughout the imaging sessions.

**Structural imaging:** High-resolution $T_2$*-weighted images, carefully planned for covering sub areas 3a, 3b and 1 of S1, were acquired using a gradient echo sequence (TR/TE=400/16 ms, 4 slices, 512 × 512 matrix, 0.068 × 0.068 × 0.500 $mm^3$ resolution).

**FMRI:** The BOLD-fMRI images were acquired from the same slices using a 2-shot GE-EPI sequence (TR=750 ms, TE=16 ms, 64 × 64 matrix, 0.547 × 0.547 $mm^2$ in-plane resolution, 2-mm thickness, 4 slices). CBV-fMRI data acquisition began 10 minutes following a slow intravenous (IV) bolus of monocrystalline iron oxide nanocolloid contrast agent (MION, 12 mg/kg). The CBV-fMRI data were acquired using the same sequence (TR = 750 ms, TE = 10 ms, 64 × 64 matrix, 0.547 × 0.547 $mm^2$ in-plane resolution, 2 mm thickness, 4 slices). Each functional imaging run consisted of 300 image frames. At least 3 fMRI runs were acquired for an individual distal digit in each session. For detailed methods, see Chen et al., 2007, 2012; Qi and Wang et al., 2016a.

**Tactile stimulation protocol for fMRI data collection:** The same stimulation protocol described by Chen et al. (2012) was used in the present study. The hand on the same side of the DC-lesion was secured in plasticine, leaving the glabrous surfaces available for tactile stimulation. Individual distal phalanges were stimulated with round-tipped plastic probes (1 mm diameter) connected to a piezoelectric vibrating stimulator, which indented the skin 0.2 mm. The stimulator was controlled by a function generator unit (Grass-Telefactor, West Warwick, RI) programmed to deliver square wave pulses with a 25 ms duration at a rate of 8 Hz, applied in blocks of 30 seconds on and 30 s off.

**Alignment:** The high-resolution T2*-weighted images revealed cortical venous distributions for locating sub areas of S1 and providing structural landmarks such as sulci and blood vessel patterns, which aided the alignment of fMRI activation map with a high-resolution photograph over the sensorimotor cortical areas and allowed verification of somatotopy and responsiveness of fMRI activations with microelectrode mappings.

### 2.4. Surgical procedures of dorsal column lesion

A unilateral DC-lesion was made with general anesthesia under aseptic conditions (see Qi et al., 2011). In brief, incisions were made into the skin and muscle to expose the dorsal vertebrae of C4-C5. A small opening was created on the dorsal arch of the vertebrae of the spinal cord, making the dura and pia covering the cervical spinal cord accessible. The DC-lesion was made with fine forceps and surgical iris scissors. The dura was then replaced by Gelfilm, and the incision site closed. Post-operative care included antibiotics (ceftiofur sodium; 2.2 mg/kg, intramuscular; every 24 h) and analgesics (buprenorphine; 0.005–0.01 mg/kg intramuscular; every 8–12 h) as previously described (Qi et al., 2011).

### 2.5. Multiunit microelectrode mappings and measures of cortical reactivation

To characterize neuronal response properties after DC-lesions and verify the somatotopy of fMRI maps with more precise microelectrodes maps, we recorded neuronal activity in the hand region of somatosensory cortex with either single tungsten microelectrodes (monkeys SM-Fy, SM-Hn, SM-Ur, SM-Ya), or arrays of 100-microelectrodes (monkeys SM-Bu, SM-Fr, SM-He, SM-Kr, and SM-Ra). To target the location of array insertion, the location of the hand region of area 3b was estimated from anatomical landmarks in three monkeys, or briefly identified in two monkeys (SM-Bu, SM-Fr) with single microelectrode mapping. Neuronal responsiveness, receptive field properties, and somatotopies with a spatial resolution around 200–400 μm in the deprived somatosensory cortex contralateral to the spinal cord lesion were determined weeks to months after the final fMRI mapping for all nine monkeys.

The surgical procedures for these terminal recording sessions have been fully described elsewhere (Reed et al., 2008; Qi et al., 2014). In brief, each monkey was sedated with a ketamine injection (10–30 mg/kg, i.m.) followed by 2–4% isoflurane gas. Each monkey was secured in a stereotaxic device and anesthesia was maintained with propofol during surgery (10 mg/kg/hr, iv) and recordings (0.3 mg/kg/hr, iv) for the duration of the experiment (24–72 h). Paralysis was maintained with vecuronium bromide (0.1–0.3 mg/kg/hr, iv) mixed with 5% dextrose and Lactated Ringer's solution, and the monkey was artificially ventilated. Craniotomy and duratomy were performed to expose the hand representation of somatosensory cortex. The electrode array was inserted into the cortex pneumatically to a depth of 600 μm, the expected depth of layer 3. All exposed cortex was covered with 1% agar mixed with Ringer's solution to provide stability and to prevent desiccation. In two monkeys, somatosensory cortex was mapped with single tungsten microelectrodes, as previously described (Merzenich et al., 1978 and Sur et al., 1982).

To obtain measures of the proportions of the area 3b hand representations that respond to touch on the hand and each of the five digits, we used NIH ImageJ v. 147 software to determine the areal sizes of the responsive hand region and the digit regions after recovery from a DC-lesion in nine monkeys. Results were compared to the sizes of the hand and individual digit territories from four monkeys without DC-lesion from another anatomical study (Liao et al., 2013). As in other studies, the border of area 3b hand cortex was determined by microelectrode mapping in all cases, and the area 3b borders were verified histologically in four of nine cases where cortex was sectioned parallel to the pia surface.

### 2.6. Extent and level of the dorsal column lesions

To determine the level and extent of the DC lesion, a transganglionic tracer cholera toxin subunit B (CTB, Sigma-Aldrich Co. LLC, St. Louis, MO) was subcutaneously injected into the tips of D1, D3, and D5 of both hands (1% in dH2O, 5 μl at each injection site) while the monkeys were anesthetized with 1–3% isoflurane. The procedures followed are those described previously by Qi and Kaas (2006), and Qi et al. (2011). The reason for injecting tracers into fingertips is because they have the highest density of receptors in the hand (Cortiani et al., 2020). To allow for appropriate transportation time, injections were placed four to six days before the terminal microelectrode mapping procedure.

The level of DC-lesion was determined by dissection results and confirmed by the relation of the lesion to labeling afferent terminal fields in the dorsal horn (Supplementary Fig. 1A – 1H). Lesions between C4 and C5 were likely above ascending inputs from all digits. Most axon fibers afferents from D1, and possibly some fibers from D2 would be spared by lesion at the level of C5 – C6. The extent of lesion was determined by reconstructing the damaged tissue from sections cut in the horizontal (coronal) plane along the length of the spinal cord (Supplementary Fig. 1a – 1h). In order to quantitate the percent of the effective DC-lesion, the CTB-labeled terminal fields in the cuneate nuclei in the brainstem were measured using NIH ImageJ v.147 software (available as freeware from https://imagej.nih.gov/ij/download.html). Detailed procedures are described elsewhere (Qi et al., 2011). The areal sizes of the CTB labeled patches of axon arbors were measured in individual brainstem sections containing the cuneate nuclei of both lesioned and non-lesioned sides. The extent of the effective lesion was calculated as the percent of the sizes of the label patches on the lesioned side compared to the non-lesioned side. All measurements were then exported to Excel software for summary and illustration purposes.

### 2.7. Tissue processing

At the conclusion of the terminal microelectrode mapping session, each monkey was given a lethal dose of anesthetic (sodium pentobarbital), and then perfused transcardially with phosphate buffered 0.9% saline (PBS, pH 7.4) followed by 2–4% paraformaldehyde in PB, and then 2–4% paraformaldehyde with 10% sucrose in PB. The brain and spinal cord were removed. In five out of nine cases, the cortex was separated from subcortical structures, manually flattened, and kept flat between glass slides (see Gharbawie et al., 2011) The cortex, brainstem, and spinal cord were stored overnight in 30% sucrose in PB for cryoprotection. The flattened cortex was cut parallel to the surface at 40 μm thickness on a freezing microtome, and the sections were stained for myelin Gallyas (1979), and cytochrome oxidase (Wong-Riley, 1979) to reveal the cortical areal boundaries related to area 3b. The brains from the other four monkeys (SM-Bu, SM-Fr, SM-Hn, and SM-Kr) were sectioned in the coronal plane for architectonic study. The brainstem was sectioned in the coronal plane and the spinal cord in the horizontal (coronal) plane, both at 40 μm thickness. Every fourth section of the brainstem and every other section of the spinal cord was immunostained to reveal the CTB label (Qi et al., 2011). Another series of brainstem sections was processed for cytochrome oxidase to reveal architecture (Qi and Kaas, 2006).

## 2.8. Data processing

**FMRI data analysis:** All data were analyzed in MATLAB (MathWorks, Natick, MA) with initial processing during acquisition. Functional data were not smoothed in the spatial domain, and the initial five volumes of each run were discarded from data analysis so that only steady state signals were included. The signal time courses were drift corrected, then temporally smoothed with a low-pass filter (0.25 Hz cutoff). Activation maps were determined using voxel-wise correlation of fMRI signal with the stimulus waveform (Chen et al., 2007). The areas of single digit activation in different brain areas were then determined using a threshold at $p < 10^{-4}$ (uncorrected for multiple comparisons) and a cluster size of $k \geq 2$. The signal time courses from significantly activated voxels in area 3b were extracted for each run within a session. Visual examination was used to select the highest amplitude voxel in activation clusters of 2 or more voxels, and stimulus-related peak signal amplitudes were obtained from the single peak voxel for summaries and comparisons.

**Longitudinal summary data (fMRI and behavior):** The fMRI peak signal change for each digit at each imaging time point for all monkey cases was arranged in long format Excel spreadsheets. When more than one run was acquired for stimulation on a given digit, the run with the largest peak signal amplitude was selected for inclusion in the summary dataset. The negative peak values from CBV were converted to positive values to allow summary with positive BOLD peak values. A subset of analyses and figures tracked the peak amplitudes of each digit, such that each run was maintained as a data point. For other analyses that tracked overall activation over time corresponding to behavioral measures, the peak amplitudes of fMRI signal change for individual digit stimulation runs were averaged into a single mean digit activation value. The behavioral data obtained for each week for each monkey was arranged in the same spreadsheet. Difference scores were calculated between values collected Pre-lesion and Post-lesion by week. To relate imaging activation to behavioral recovery, variables were coded to group weeks into periods that corresponded to the imaging dates (Post-1: week 1–4; Post-2: week 5–8; Post-3: week 9–12). The identity of each monkey, training group, and lesion information were associated with the fMRI activations, task success scores for each well, and task trajectory measures in the spreadsheet. The spreadsheet was imported into IBM-SPSS software for descriptive statistics, correlations, and generalized linear modeling analyses. An additional variable to group cases based on the DC-lesion was determined post-hoc after reviewing the data and assessing best fit of fMRI activation for groupings of 2 and 3 (e.g., < 90% and ≥ 90%; less than 70%, between 70–90%, 90% or greater) with generalized linear modeling.

## 2.9. Data analysis and statistics

**Labeled axon terminal fields:** Statistical comparisons between measures of the terminal fields in the sections of the cuneate nuclei from both intact and deprived sides were performed with the Wilcoxon matched-pairs signed-ranks test ($\alpha = 0.05$) using GraphPad Prism software (GraphPad software Inc.).

**Behavioral data analysis:** GraphPad Prism software was used with a Kruskal-Wallis Test (Nonparametric ANOVA) followed by Dunn's Multiple Comparisons Test to compare

success score and kinematic trajectory of hand use in the reach-to-grasp task before and after DC-lesion in each monkey.

**Total mean rank:** We ranked the behavioral recovery performances of monkeys based on several factors. (1) The numbers of post-lesion days when monkeys were first able to retrieve pellets with impaired hands from testing wells and further behavior testing became possible. (2) Mean differences between post- and pre-lesion values in total success score (% of success and the number of digit flexes) for up to 12 weeks post-lesion testing; (3) Mean differences between post- and pre-lesion values in Time, Distance, and Speed during Reach, Grasp, and Retrieval segments. The total rank was calculated from the average of all these categories. We refer to the behavioral outcome as total mean rank throughout the entire manuscript. No success scores and kinematic measures were available for SM-Bu and SM-Hn, thus, they were excluded from these rankings. For the overall comparison, we assigned the ranks based on the initial day rank and average ranking of all other monkeys.

**FMRI data analysis:** We performed several analyses. (1) We tested the distributions of measured values in relation to a normal distribution using the 1-sample Kolmogorov-Smirnov test, and in relation to each condition using 2-sample Mann-Whitney U-test and Kruskal-Wallis test for more than two conditions. For example, we compared the distributions of BOLD and rectified CBV response amplitudes. Additionally, the differences were taken between pre-DC-lesion and post-DC-lesion values of the primary measures to standardize values for each monkey, and compared to the distributions of difference values between the pre-DC-lesion and post-DC-lesion responses in our samples. (2) To test expectations that the magnitudes of responses to the stimulation of each digit are similar for all digits before DC-lesion but may change after DC-lesion if the lesion spares D1, we selected the percent fMRI signal change in response to D1 stimulation as a reference to be compared to stimulation on each digit. These ratios were calculated for each monkey within each scan session.

**Longitudinal summary data analysis:** We used the difference values of primary measures before and after the DC-lesion to relate behavioral measurements to brain activation. (1) To correlate fMRI results with behavioral results, we first computed the mean percent of signal change using the best digit responses from all runs of each scan, and then computed the means of rectified differences from pre-lesion scans. Then, the difference values of peak responses from all digits stimulated in a session were averaged to provide one value. Each peak response difference was matched to the corresponding single difference value for the given behavioral measure averaged over the corresponding scan time period. We then performed Pearson's correlations (r) and linear regression. (2) To determine if the reactivation of digits 1, 2, or 3 more strongly predict behavioral recovery, for the final fMRI scan period (weeks 9–12), we plotted the difference values of peak responses for digits 1, 2, and 3 separately against the overall behavioral performance rank for each monkey and obtained the coefficient of determination $R^2$ from linear regression. (3) For relationships between lesion extent, behavioral measurements, and fMRI percent signal change, we used the difference values of the primary behavior measures and the peak response average from all of the digits combined to perform linear regressions, evaluating the therapy groups

together. (4) To test how the task-specific therapy affects each measure, generalized Linear modeling (GLM) was performed with Bonferroni correction for multiple comparisons, using DC-lesion, therapy, and recovery time as fixed effects. Models for a given response variable were selected based on the lowest Akaike Corrected Information Criterion.

Measurements, difference values, and ratios were calculated in Excel, and then imported into SPSS for distribution statistics, generalized linear regression, and mixed modeling analyses. Summary figures were generated in Excel, SPSS, or MATLAB and then edited in Adobe Illustrator.

## 3. Results

The time course of recoveries from dorsal column lesions (DC-lesions) were evaluated with longitudinal measures of behavior and cortical reactivation in monkeys with or without intensive behavioral therapy. The final fMRI activations were compared with microelectrode mappings. We determined the relationship between extents of DC-lesions, the dexterity of hand use, the progression of fMRI responses over time, and the recovery of somatotopy and neural responsiveness. Note that for ease of comparison, some of the images and reconstructed maps from the cortex contralateral to unilateral DC-lesions have been reversed to the view of the left hemispheres.

### 3.1. Measures of lesions for each case

The percentage of spared axons from the digits depended on the levels and the extents of the DC-lesions. The histological results indicate that incomplete DC-lesions were placed at spinal cord cervical segments at the border between C4 and C5 for monkey SM-Ra; at the rostral potion of C5 for monkey SM-Kr; at C5 for monkeys SM-Bu, SM-Fr, SM-Fy, SM-Ur; and at the borders between C5 and C6 for monkeys SM-He, SM-Hn, SM-Ya (Supplementary Fig. 1). The results from our quantitative measurements of spared axon terminals in the cuneate nucleus (see Fig. 2A and 2B as examples) indicate that the completeness of DC-lesions (based on losses of inputs from digits 1, 3, 5) for the monkeys included in this study ranged from 64% to 91%. The summed areal differences of the CTB labeled terminal fields in the cuneate nuclei between lesion and non-lesion sides were highly significant (Wilcoxon matched-pairs signed-ranks test, $p < 0.001$). As shown in Fig. 2A, there was almost total absence of CTB-labeled axon terminals to the lesioned cuneate nuclei in squirrel monkey SM-Fr (91% complete). Likewise, labeled axon terminal fields were largely reduced in the lesioned cuneate nuclei in squirrel monkey SM-Bu (82% complete, Fig. 2B). For other cases, see Table 1. For white matter damage, the lesions in six out of nine monkeys (SMs-Bu, Fy, Kr, Ur, He, Hn) were restricted to the dorsal column and spared the corticospinal tract (CST), which is one of the major motor pathways involved in controlling dexterity in non-human primates. The DC-lesions for monkeys SM-Ra and SM-Fr extended also into a small portion of the CST (Supplementary Fig. 1b, 1i), which appeared to result in some motor deficit and difficulty controlling manual dexterity. In two monkeys (SM-Fr and SM-Ya), the white matter damage also involved the reticulospinal tract located in the most medioventral portion of the spinal cord, which may have also contributed to the control of grasp movement of hand (see Discussion). For gray matter damage, we found that DC-lesion

also involved various extents of gray matter that encroached into the intermediate zone and ventral horn at the lesion level in all monkeys. Damage to this part of spinal cord may also affect the control of dexterity. Damage to the dorsal column occurred in all monkeys in the injury group, and this is reflected in the somatosensory activation patterns in fMRI.

### 3.2. Behavioral impairments and recovery with or without intensive behavioral therapy after dorsal column lesion

We assigned five monkeys for the intensive behavioral therapy group and four in the minimum behavioral therapy group. Two monkeys (SM-Bu and SM-Hn) from the second group lost their interest in sugar pellets over time, therefore we used other food items to maintain their task performance, but these data were not suitable for quantification. Nevertheless, systematic observations were made to detect when monkeys were able to start to retrieve small treats (e.g., pieces of peanuts, marsh-mallows) from testing board or testing wells. Thus, we were able to track when the two monkeys were first able to retrieve food items from testing wells with the impaired hand. Quantitative measures for the other seven monkeys were used to characterize the degree of impairment and subsequent recovery of hand use in the reach-to-grasp task. We refer to “success scores” as a category including the following two measures: percent of successful trials, and number of digit flexes (attempts) per successful retrieval. We used “kinematic measures” to refer to nine features of the behavioral task which included the duration, distance, and speed of hand movements during reach, grasp and retrieval segments. Kinematic data from six out of seven monkeys were analyzed and included in this study, but kinematic analysis from monkey SM-Fy was not available due to a video problem. Note, all nine monkeys were successfully imaged and evaluated histologically.

#### 3.2.1. Relationship between behavioral impairment and severity of DC-lesion, and therapy

**Success scores.:** Our task-related behavioral testing indicated that success scores before the lesion were similar for all four wells (of increasing depths and difficulties) for all tested monkeys ($n = 7$); further, digit flexes (attempts) were comparable for W1 - W3 but were only marginally higher for W4. Thus, the intact monkeys were equally proficient in retrieving sugar pellets from shallow to the deepest well.

Post-lesion, initial impairments on the affected hand were apparent in all tested monkeys. These deficits were reflected by decreased mean success scores and increased mean number of attempts per successful trial (GLM Pre – Post-1: Success $X^2 = 101.283$, Bonferroni adjusted $p = 2.92 \times 10^{-9}$; Attempts $X^2 = 158.519$, adjusted $p = 1.82 \times 10^{-12}$). The deficits were more prominent for more difficult wells W3 and W4 (Fig. 3, Supplementary Fig. 2). In monkeys with a more extensive lesion (i.e., larger than 90%), a deficit was clearly present for both difficult wells (W3 and W4) and easier wells (W1 and W2), for both intensive and minimum behavioral therapy cases (Fig. 3, Supplementary Fig. 2). In the generalized linear modeling, the three categories of lesion completeness had a significant main effect on the difference in number of attempts per success for the most difficult well (GLM: Attempts $X^2 = 70.905$, $p = 4.441 \times 10^{-16}$), and there was a weak effect on the percent success (GLM: Success $X^2 = 4.834$, $p = 0.089$). Results from Non-parametric Kruskal-Wallis ANOVA

with Dunn's multiple comparisons tests indicated that significant post-lesion declines in the success scores were detected in some cases (stars in Fig. 3A, Supplementary Fig. 2A, 2C, 2G), and significant increases of attempts after lesion were detected for most of the cases (stars in Fig. 3B and 3G, Supplementary Fig. 2B, 2D, 2F, 2H). Note, the observations for each lesion category were not equal (lesion <70% $n = 39$, intermediate $n = 48$, lesion >90% $n = 115$ behavioral testing scores), due to the range of lesions in the seven monkeys with quantified task performance.

Training alone (as a main effect) did not reach significance as a predictor of percent success (GLM: $X^2 = 1.379$, $p = 0.240$) or attempts (GLM: $X^2 = 0.229$, $p = 0.632$) considered across all time points; however, there were fewer measures from minimum therapy cases (observations: non-trained $n = 63$; trained $n = 139$). The interaction between lesion extent and post-lesion recovery time had a strong influence on attempts per success on difficult wells, but over time the therapy condition had a weaker effect (GLM: Lesion x Recovery Time $X^2 = 102.295$, $p = 0.0001$; Training x Recovery Time $X^2 = 17.719$, $p = 0.001$) because all cases improved after the Post-1 period. The data suggested that a trend for earlier recovery of dexterity in hand use for the intensive therapy group with a significant difference in digit flexes at 2–4 weeks (adjusted $p = 1.586 \times 10^{-9}$) based on Kruskal-Wallis testing of digit flexes in each monkey. However, the time of recovery for most monkeys began around post-lesion week 6–7 and appeared to stabilize by post-lesion weeks 9–12 in both groups.

**Kinematics measures of hand movement.:** Nine measures of hand movement during the reach-to-grasp task were collected and analyzed for the first five successful trials from well 1. After DC-lesions, the majority of trained and minimum therapy monkeys showed clear deficits in hand movement during the task, as reflected by longer distances and time of hand movements, and slower speeds than pre-lesion for completing all three segments (Fig. 3 and Supplementary Fig. 3). From GLM, the three lesion categories had a significant main effect on the difference in time to complete reach, grasp, and retrieval (Time: Reach $X^2 = 104.963$, $p = 0.0001$; Grasp $X^2 = 18.952$, $p = 1.34 \times 10^{-5}$; Retrieval $X^2 = 101.885$, $p = 0.0001$). Similarly, the speed (velocity of movement) for task completion post-lesion was slower (Speed: Reach $X^2 = 9.860$, $p = 0.002$; Grasp $X^2 = 32.802$, $p = 1.02 \times 10^{-8}$; Retrieval $X^2 = 49.763$, $p = 1.74 \times 10^{-12}$). The lesion extent had significant main effects on distance of reach and retrieval components (Distance: Reach $X^2 = 37.482$, $p = 9.23 \times 10^{-10}$; Grasp $X^2 = 0.732$, $p = 0.392$; Retrieval $X^2 = 6.708$, $p = 0.010$).

As shown in details in Fig. 3 and Supplementary Fig. 3, the time was significantly longer in monkeys SM-Fr and SM-Ra ($p < 0.001$), SM-He and SM-Ur ($p < 0.01$), SM-Ky ($p < 0.05$). Similarly, the post-lesion speed (velocity of movement) for completing reach and grasping segments was significantly slower in monkey SM-Fr ($p < 0.001$), and initially significantly slower in reach ($p < 0.001$) and grasping ($p < 0.05$) in monkey SM-Ra. The speed did not significantly changed in monkeys SM-He, SM-Kr, SM-Ur, and SM-Ya. Post-lesion Distance to complete all three segments was initially significantly longer for monkeys SM-Ur ($p < 0.001$) and SM-Kr ($p < 0.01$). There was no significant change for all other monkeys (Fig. 3, Supplementary Fig. 3). The results also demonstrate a trend between lesion extent and severity of impairment, such that extensive lesions resulted in longer distances, longer times, and slower speeds of hand movement in the reach-to-grasp task (Fig. 3, Supplementary

Fig. 3). However, these kinematic impairments were not permanent, as they returned toward pre-lesion levels when tested around post-lesion weeks 6 – 12.

Although the severity of the behavioral deficits correlated with lesion extent, cases with intensive therapy were associated with the recovery of some aspects of the hand movements during reach and retrieval. Over all the cases, the results suggested that intensive therapy shortened the distance and time durations for reach, grasp, and retrieval (GLM Therapy: Reach Distance $X^2 = 59.211$, $p = 1.421 \times 10^{-14}$; Grasp Distance $X^2 = 6.944$, $p = 0.008$; Retrieval Distance $X^2 = 37.642$, $p = 8.501 \times 10^{-10}$; Reach Time $X^2 = 104.963$, $p = 0.0001$; Grasp Time $X^2 = 18.952$, $p = 1.34 \times 10^{-5}$; Retrieval Time $X^2 = 101.885$, $p = 0.0001$) and increased the reach and retrieval speeds (Reach Speed $X^2 = 13.384$, $p = 2.53 \times 10^{-4}$; Grasp Speed $X^2 = 2.691$, $p = 0.101$; Retrieval Speed $X^2 = 10.856$, $p = 0.001$).

**Initial day to perform the task.:** We used the term ‘initial day’ for the number of post-lesion days when monkeys were first able to retrieve pellets with the impaired hands from the testing wells. In general, monkeys with intensive therapy were able to perform the tasks earlier than minimum therapy monkeys even when DC-lesions were extensive (Fig. 4A). Behavioral recovery also depended on the lesion extent, such that monkeys with less extensive lesions had better and/or earlier recoveries than those monkeys with more extensive lesions. In contrast, two monkeys (SM-Bu and SM-Hn) who were unmotivated to perform the Kluver board task had poor behavioral recovery. SM-Bu took 83 post-lesion days to retrieve food items from the easy well (W1), and 133 days from the most difficult well 4 (Fig. 4A), despite this monkey having a less extensive DC-lesion (82% complete). This contrast suggests the potential power of early rehabilitative intervention for accelerating behavioral recovery. The relationship between lesions and overall behavioral outcomes represented by ranking is illustrated in Fig. 4B – 4D. As shown in Fig. 4C, SM-Bu (82% complete, minimum therapy) was most impaired in overall ranking, followed by SM-Ur (86% complete, intensive therapy), SM-Ra (>90% complete, minimum therapy), SM-Fr (91% complete, intensive therapy), SM-Hn (64% complete, minimum therapy), SM-Fy (73% complete, intensive therapy), SM-Ya (65% complete, intensive therapy), SM-Kr (90 % complete, intensive therapy), SM-He (86% complete, minimum therapy). To track changes in behavioral recovery over time, we plotted the DC-lesion completeness as a function of mean kinematic rank for six monkeys. No kinematic measures were available for SM-Bu, SM-Fy, and SM-Hn, thus, they were excluded from this comparison. As shown in Fig. 4D and Supplementary Figure 4, all monkeys improved on the food retrieval task over testing time regardless of lesion size and task experience. The one exception (SM-He) had a smaller lesion and started at a high level of performance, improved slightly, and then regressed. This is one of two monkeys with only testing experience (minimal therapy). The other monkey with only testing experience (SM-Ra) had a somewhat larger lesion, performed poorly on first testing, improved to a middle level of recovery, and failed to improve further. Thus, some improvement can occur over time with only testing experience. Other monkeys with extensive task experience, improved two ranks to a high level with a smaller lesion (SM-Ya), and nearly two ranks after the largest lesion (SM-Fr), or less than one rank but to a high level after a large lesion (SM-Kr), suggesting that intensive therapy can lead to high levels

of performance after even large lesions, but not always as monkey SM-Ur with 86% lesion improved only slightly (Fig. 4D).

At the early stage of recovery, there was no clear relationship between the lesion extent and mean ranking of kinematic measures, and monkeys in the therapy condition were not superior. Over longer recovery times, the relationship between kinematic rank and lesion extent become stronger ($R^2$ = 0.215). By post-lesion week 9–12, there was an even stronger relationship ($R^2$ = 0.396) between kinematic rank and lesion extent. This stronger relationship over time between kinematic rank and the lesion reflects the poor initial performance of monkeys and improvements over time, but the lesion completeness limits the recovery, regardless of behavioral therapy. Thus, as expected, monkeys with the most complete lesions took longer to recover, and recovery was less complete. Nevertheless, 3 out of 4 monkeys in the intensive therapy group exceeded the performance of the monkeys in the minimum therapy group.

In summary, intensive therapy of the impaired hand promoted the recovery process, but with some limitations. We found that extensive DC-lesions produced a higher degree of impairment in the reach-to-grasp task, and that task-specific therapy contributed to earlier hand use recovery when injuries were incomplete. There was a trend for an earlier recovery of dexterity in hand use for the intensive therapy group with a significant difference in digit flexes at 2–4 weeks. The time of recovery for most monkeys began around post-lesion weeks 6–7 and appeared to stabilize by post-lesion weeks 9–12 in both groups. Intensive therapy significantly improved aspects of post-lesion distance, time, and speed of task performance, but intensive therapy alone did not overcome all impairment aspects measured here after extensive DC-lesions.

**3.2.2. Lesions that involved a portion of motor pathway—**In two monkeys (SM-Fr and SM-Ra), an extensive DC-lesion (est. 91% and >90%, respectively) encroached into a small portion of cortical spinal tract (CST, blue arrows and contours in Supplementary Fig. 1b, 1i); note the CST is a major motor pathway for controlling dexterity in non-human primates (e.g., Sugiyama et al., 2013; Schmidlin et al., 2004). The behavioral analysis indicated the deficits of these two monkeys, as reflected by the kinematics measures, were greater than most of the other monkeys with lesions restricted to the dorsal columns. In the post-lesion testing, both the time and speed to complete all segments were significantly longer or slower than measured before the lesion. Fig. 3 (C – E, H – J) shows examples of behavioral impairment and recovery after DC-lesion for monkeys SM-Fr and SM-Ra. This severe kinematic deficit affecting hand movements suggest that the combination of an extensive DC-lesion (>90%) plus CST damage were the two main factors contributing to an abnormally longer time for task completion, and an overall slower speed of hand movement during the task performance. Notably, even with a similar extent of the DC-lesion with a partially damaged CST, the intensive therapy monkey SM-Fr was able to retrieve pellets from the most difficult well (W4) at week 2 post-lesion, while the minimum therapy monkey SM-Ra was only able to retrieve pellets from W4 at week 4 post-lesion. This result again suggests that early intervention may accelerate the rate of behavioral recovery of hand use. However, with only two cases reported here, further study is needed.

### 3.3. FMRI signal changes from hand cortex after DC

**3.3.1. BOLD vs. CBV signals—**Two types of fMRI responses were collected in the present study: blood oxygen level dependent (BOLD, six monkeys) and cerebral blood volume (CBV, three monkeys) with monocrystalline iron oxide nanoparticles (MION) enhancement. Since the peak response of BOLD and CBV were opposite in value, the absolute value of the negative CBV peak signal changes were used for comparison with positive BOLD peaks. CBV had larger peak magnitudes across all pre- and post-lesion periods (e.g. for Pre, $U = 716$, $p = 0.0001$; CBV rank = 45.1, BOLD rank = 21.66). However, there was no significant difference when using difference scores from pre-lesion values between CBV and BOLD percent signal change variables ($p = 0.8$). The present study focused on the fMRI signal within the region of interest (ROI) where foci in the hand region of somatosensory area 3b contralateral to the side of DC-lesion were activated by vibrotactile stimulation of the digits. Foci of fMRI signals outside of the sensorimotor areas were not included in the composite fMRI maps. However, examples of raw images are presented in Figs. 6 – 8 and in the supplemental material (Supplementary Figs. 5 – 6).

**3.3.2. Lesions reduce fMRI response magnitudes—**The effects of DC-lesions on the magnitudes of the fMRI responses in the hand region of area 3b were evaluated over the recovery process. Fig. 5 (A and B) illustrates CBV signals from significantly activated voxels in area 3b to vibrotactile stimulation on distal phalanges of digits 1 and 3 before and four times after a DC-lesion for squirrel monkey SM-Ya. This monkey had a large section of unilateral dorsal column at a slightly lower cervical level (at the border between C5 - C6), to spare most of peripheral inputs from D1, and possibly some from D2, due to inputs entering the spinal cord above the DC-lesion. Inputs from D3 - D5 below the lesion were mostly interrupted (Supplementary Fig. 1H, 1h). As inputs to the cuneate nucleus were mostly spared from D1, peak amplitudes of signal changes for stimulating D1 at 4, 6, 8, and 12 weeks after the DC-lesion were similar to that of the pre-lesion level (Fig. 5A). In contrast, peak amplitudes of signal change for stimulating the mostly lesioned input from D3 varied but all were lower than that of pre-lesion level, with the lowest peak response amplitude found at post-lesion week 6. By post-lesion weeks 8 and 12, the peak amplitudes gradually increased, but were still lower than that of the pre-lesion level (Fig. 5B). Note that peak response amplitudes varied over imaging sessions even for the stimulation of the mostly spared D1. While many factors may influence fMRI responses profiles, including anesthesia level, the post-lesion reduction in the peak response amplitudes recorded while stimulating D3 most likely reflected the effect of DC-lesion.

To summarize fMRI response magnitudes before and at times after DC-lesions from BOLD MRI or CBV MRI groups, response magnitudes of BOLD or CBV signals for voxels significantly activated by vibrotactile stimulation for each digit were extracted and averaged across runs within a session and across sessions for all monkeys. As shown in Fig. 5C and 5D, although the overall magnitudes were different between CBV (absolute value) and BOLD responses, they follow the same trend in which averaged peak responses initially decreased from pre-lesion levels at post-lesion weeks 2 – 4 and then returned toward pre-lesion levels when measured during post-lesion weeks 5 – 8.

Due to the variation of lesion extents, we grouped cases into three categories: nearly complete lesion (>90% complete), large lesion (73% - 86% complete), and less extensive lesion (64% - 65% complete).

**Cases with a nearly complete lesion.:** Blood oxygen level dependent (BOLD) functional activations were obtained using high resolution 9.4T MR scans to reveal responses in area 3b to tactile stimulation on distal digits before and after DC-lesions. Monkey SM-Fr had a unilateral 91% complete DC-lesion on the left side of cervical spinal cord C5 (Fig. 2A, 2C), sectioning nearly all of the direct inputs from D1 - D5 to the cuneate nucleus. This monkey underwent intensive therapy of the impaired hand for three months, and the terminal electrophysiological mapping was conducted at post-lesion week 70. The pre-lesion BOLD responses to tactile stimulation of D1 - D5 detected were roughly arranged in a lateromedial progression in the hand region of area 3b (not shown), reflecting the normal somatotopy (Sur et al., 1982). Two weeks after the DC-lesion, focal activations to the 8 Hz vibrotactile stimulation of D1, D2, and D4 were detected in area 3b, however the locations were some-what abnormal. At post-lesion week five, digit somatotopy was abnormal. At post-lesion week eight, a nearly normal somatotopic sequence of reactivations of area 3b by digit stimulations occurred even after a loss of 91% of inputs from digits due to the DC-lesion in this monkey with intensive therapy.

Similarly, squirrel monkey SM-Kr had a unilateral 90% complete DC-lesion on the right side of cervical spinal cord C4 - C5. This monkey underwent intensive therapy of the impaired hand for three months, and the terminal electrophysiological mapping took place at post-lesion week 26. Pre-lesion, BOLD responses to tactile stimulation of all five digits were detected in the hand region of area 3b reflecting the normal somatotopy (not shown). After four weeks of recovery, BOLD responses to tactile stimulation of D1 and D2 were in locations similar to the pre-lesion responses. By post-lesion week nine, multiple response foci for D1 and D5 in area 3b were detected in lateral and medial locations which resembled the normal pattern. However, the responding foci from D3 were shifted medially, and the responses to D2 and D4 were not detected altogether. Thus, the somatotopy of fMRI activations after extensive DC-lesions remained abnormal. While extensive lesion in both cases produced reduced and abnormal activation patterns, only case SM-Fr returned to near normal patterns, despite both undergoing intensive therapy.

**Cases with a large lesion.:** Squirrel monkey SM-Bu had an extensive but incomplete unilateral DC-lesion (82% complete) on the right side of cervical C5 (Supplementary Fig. 1A, 1a) that spared some inputs from D1 - D5, which were detected after CTB tracer was injected into the distal phalanges of three digits (Fig. 2B, 2D). Although D2 and D4 were not injected with CTB tracer, some inputs were likely spared from these two digits. Before DC-lesion, the foci of CBV signal in area 3b in response to vibrotactile stimulations of D1 - D4 were robust, and arranged in a lateromedial sequence (Fig. 6) that reflected the normal representational territories of these digits. Note that D5 was not stimulated. Four weeks after the DC-lesion, the CBV signals in area 3b in response to tactile stimulation on the contralateral distal D1 (red), D2 (blue), D3 (yellow) and D4 (green) were scattered and weak, but the locations of these response foci roughly resembled pre-lesion foci. At week

6 post-lesion, the CBV map was similar to the week 4 post-lesion map. In addition, some response foci also appeared in the hand regions of areas 3a and 1 (Fig. 6). After eight weeks of recovery, a focused response for D1 and multiple foci of responses for D3 and D4 were detected in areas 3a, 3b and 1. However, a response from D2 was not detected in this scan session (Fig. 6). Overall, the somatotopy of the D1, D3, and D4 foci was less precisely organized in area 3b than that of normal monkeys in this case with minimal therapy.

The other CBV-scanned monkey (SM-Fy) in this group had a less extensive DC-lesion (73% complete) on the left side of cervical C5 and had intensive therapy for three months post-lesion. The lesion in the spinal cord was slightly more lateral than in other cases, such that some afferents from the hand were left uncut by the DC-lesion (Supplementary Fig. 1C, 1c). The pre-lesion foci of CBV responses in area 3b to tactile stimulations of D1-D4 were present and arranged in a normal lateromedial sequence (Fig. 7). The fMRI scans at weeks 4, 6, and 9 post-lesion revealed the CBV responses to tactile stimulation on contralateral distal D1 - D4 were mostly detectable in area 3b. However, there were no responses detected from D2 in week 2 post-lesion scans. Overall, the CBV-responses from stimulating D1 – D3 were in normal sequence at post-lesion week 6 (Fig. 7).

Both squirrel monkeys SM-He and SM-Ur had similar extents of unilateral DC-lesions (86% complete) but at slightly differing levels of the cervical cord (see Supplementary Fig. 1E for SM-Ur, 1F for SM-He). Squirrel monkey SM-Ur received intensive therapy, while SM-He had minimum therapy but was tested on the same behavioral task.

BOLD responses were collected for both monkeys. The pre-lesion BOLD responses to tactile stimulations of distal digits were detected, and the somatotopy in the hand region of area 3b reflected the expected, normal pattern (see Supplementary Fig. 5 as an example). In SM-He, weeks 4 and 10 post-lesion scans registered BOLD responses from stimulation of D1 - D4 in the hand region area 3b, with a somatotopy in a nearly similar pattern to those of normal monkeys (Supplementary Fig. 5). In SM-Ur, the post-lesion scan at 4, 6, and 8 weeks reveal focal activations to tactile stimulation of some digits. However, the locations of digit activations shifted without a clear somatotopic order. By 12 weeks of recovery, focal activations to D1 - D3 were detected in locations closer to those of pre-lesion activations.

**Cases with less complete lesion.:** The two monkeys included in this group, SM-Ya (65% complete) and SM-Hn (64% complete) had large DC-lesions at a slightly lower cervical level (C5 - C6) that spared DC inputs from D1 and possibly most of D2. DC inputs from D3 - D5 were below the lesion and were mostly interrupted (see Supplementary Fig. 1G and 1 g for SM-Hn, Fig 1H and 1h for SM-Ya). Squirrel monkey SM-Ya received intensive therapy, and SM-Hn had minimum therapy. CBV responses were collected from SM-Ya, while BOLD responses were collected from SM-Hn. In monkey SM-Ya, CBV responses to tactile stimulations on the spared D1 and D2 were robust and resembled normal somatotopy, and more importantly, they consistently appeared in the hand region of area 3b throughout post-lesion weeks 4, 6, 8, and 12 (Fig. 8). Thus, the robust, longitudinal CBV responses from spared digits were consistent with spared peripheral inputs detected anatomically (see Fig. 2C in Liao et al., 2016). In contrast to D1 and D2, CBV responses to vibrotactile stimulation on the mostly deprived D4 and D5 were less robust, and the locations of

activation foci varied across post-lesion scans. After eight weeks of recovery, stimulation of D1 produced both a strong activation patch in the D1 territory and a significant CBV activation patch in a more medial location in the deprived D5 territory (Fig. 8). Thus, the D1 and D2 territories remained activated at normal levels, as expected, responses to D4 and D5 were depressed and variable, and D1 activated a second abnormal location in the D5 territory.

Squirrel monkey SM-Hn had a DC-lesion that was similar to that of SM-Ya. Axon tracing results indicated that the inputs from D1 were mainly spared, as expected, and that some fibers from D3 and D5 survived the DC-lesion (not shown). In the pre-lesion scan, foci of BOLD responses to tactile stimulation on D1 – D5 were detected in a roughly normal lateromedial sequence in the hand region of area 3b (Supplementary Fig. 6). However, the focus of D1 activation was more caudal than expected. Surprisingly, at week 2 post-lesion, the BOLD response to tactile stimulation on all digits were present in the hand region of area 3b, and the somatotopy of D1 – D4 was in a normal lateromedial progression, although the D5 response was shifted laterally somewhat. All responding patches were shifted medially compared to those of pre-lesion. After five- and eight-weeks recovery, the BOLD responses evoked by tactile stimulation on spared D1 and D2 were robust, and somatotopies of D1 – D3 remained in lateromedial order throughout post-lesion weeks 2, 5, and 8 (Supplementary Fig. 6). However, responses to stimulation of the highly deprived D4 – D5 were either not detectable in area 3b or they appeared in various shifted locations. Thus, these somewhat abnormal BOLD response patterns of SM-He were similar to those of CBV responses in squirrel monkey SM-Ya.

In summary, the somatotopic order of fMRI responses to digit stimulations in monkeys with nearly complete DC-lesions returned to resemble those of pre-lesion patterns after 8 – 9 weeks of recovery. In monkeys with incomplete DC-lesions, the somatotopies of fMRI responses returned to resemble those of pre-lesion patterns after 4 weeks of recovery. In monkeys with lesions at slightly lower levels in cervical spinal cord (C5 – C6), fMRI responses to stimulations on spared digits (D1 and D2, possibly D3) were robust and organized in somatotopic order after 2 – 4 weeks of recovery, and the responsiveness and somatotopies remained stable throughout post-lesion scans. However, fMRI responses to stimulation of the mostly deprived digits D4 – D5 varied or they appeared in various shifted locations in the hand region in area 3b over post-lesion scans.

### 3.4. Relationships of fMRI responses, lesion extent, and therapy

To summarize results across all of the cases, the reduction of the mean fMRI responses for all digits after DC-lesion significantly correlated with the percent of DC-lesion, when matched for the amount of time of post-lesion recovery (Partial correlation $r = -0.412$, $p = 0.017$, $n = 34$ observations from $N = 9$ monkeys). Statistical modeling significantly predicted the difference in post-lesion mean fMRI responses as a result of lesion category as the largest main effect (GLM Lesion: $X^2 = 12.586$, $p = 0.002$), along with the recovery time period post-lesion (GLM Recovery Time: $X^2 = 12.516$, $p = 0.006$). The therapy condition had a weaker but significant main effect (GLM Therapy: $X^2 = 7.594$, $p = 0.006$). All interactions between these three factors significantly contributed to the variation in fMRI

percent signal difference values, including the three-way interaction, which was strongest overall (GLM Lesion x Recovery Time x Therapy: $X^2 = 23.013$, $p = 3.36 \times 10^{-4}$). However, pairwise comparisons related to training conditions were not significantly different with Bonferroni adjustment. Across all recovery time periods, the interaction of the lesion with the therapy condition related to significant differences in fMRI signal changes (GLM Lesion x Therapy: $X^2 = 19.740$, $p = 5.17 \times 10^{-5}$). The effect was found in pairwise comparisons when cases had large lesions ($p = 3.49 \times 10^{-5}$) and nearly complete lesions ($p = 0.025$). Therapy did not have a significant effect when the lesion was less complete ($p = 1.0$).

Lesion completeness and time of recovery had a significant interaction (GLM Lesion x Recovery Time $X^2 = 16.500$, $p = 0.011$), but pairwise comparisons did not survive Bonferroni adjustment. This interaction of lesion category and recovery time period affected most measures of hand use (Success: $X^2 = 73.108$, $p = 9.40 \times 10^{-14}$; Attempts: $X^2 = 102.295$, $p = 0.0001$; Reach Time $X^2 = 147.425$, $p = 0.0001$; Grasp Time $X^2 = 31.247$, $p = 7.54 \times 10^{-7}$; Retrieval Time $X^2 = 115.145$, p = 0.0001; Reach Distance $X^2 = 56.877$, $p = 2.73 \times 10^{-12}$; Grasp Distance $X^2 = 42.208$, $p = 3.624 \times 10^{-9}$; Reach Speed $X^2 = 52.164$, $p = 2.76 \times 10^{-11}$; Grasp Speed $X^2 = 99.634$, $p = 0.0001$; and Retrieval Speed $X^2 = 373.410$, $p = 0.0001$). This corresponds to the tendency of less deviation from pre-lesion measures for less complete lesions, and more improvement after the first several weeks (post-1) when lesions were of intermediate severity.

While recovery time period and therapy condition related to the fMRI percent signal differences (GLM Time x Recovery Therapy: $X^2 = 9.074$, $p = 0.028$), pairwise comparisons of therapy effects at each post-lesion time were not significant. The largest difference, however, was at the post-2 time period, indicating a tendency for cases with training to improve fMRI signal changes to those closer to pre-lesion levels in the period of week 5–8. This interaction of recovery time and therapy condition affected several behavioral measures (Attempts: $X^2 = 17.719$, $p = 0.001$; Reach Time $X^2 = 19.393$, $p = 2.27 \times 10^{-4}$; Reach Distance $X^2 = 63.032$, $p = 1.32 \times 10^{-13}$; Grasp Distance $X^2 = 12.706$, $p = 0.005$; Retrieval Distance $X^2 = 60.096$, $p = 5.61 \times 10^{-13}$; Reach Speed $X^2 = 20.417$, $p = 1.39 \times 10^{-4}$; and Retrieval Speed $X^2 = 77.332$, $p = 1.11 \times 10^{-16}$). This corresponds to the tendency of less deviation from normal pre-lesion measures for the intensive therapy condition, with more improvement after the first 1–2 months (post-2), and similar improvement by 3 months (post-3). Overall, the task-specific intensive therapy tended to promote earlier improvements in aspects of dexterity and an earlier cortical recovery, even when the lesion was extensive. All cases improved if the injury was incomplete.

Additionally, within each scan session for each case, we compared the signal magnitudes in response to stimulation of D1 compared to the other digits as a difference value. This measure indicates when the activations were strong, weak, or similar in reference to D1, but without direct reference to the magnitude of D1 activation at each scan (Fig. 9). We hypothesized that when the lesion spared D1 inputs, activations to other digits would be weaker for initial post-lesion times with possible recovery to similar activation strength by weeks 9–12. The measure also shows the variation in signal magnitudes for each digit stimulated within each scan time. In our sample, at post-lesion times, this difference measure indicated when all the digits had similar levels of activation versus when D1 and D2 were

preferentially reactivated due to lesion location. As shown in Fig. 8 for SM-Ya, after a DC-lesion at a slightly lower level in the spinal cord (i.e., C5 – C6), the longitudinal fMRI responses from the stimulation of spared D1, as well as D2, were robust and greater than those of other digits. This was well reflected by anatomical tracing results indicating that axon fibers from D1 were mostly spared on the same monkey (e.g., Fig. 2C in Liao et al., 2016). Across cases, we found fMRI responses from spared digits could be detected as early as week 2 post-lesion. However, fMRI responses to stimulation of the most deprived D3 – D5 were varied in the hand region in area 3b over post-lesion weeks.

### 3.5. Correlations of lesion extent, behavioral impairment and recovery, and the fMRI response

We determined that the lesion extent was significantly, but modestly, correlated with both the fMRI response differences ($r = -0.412$, $p = 0.017$). Most of the difference measures for kinematics variables were modestly correlated with the mean fMRI measures in partial correlations controlling for recovery time, similar to the fMRI correlation with lesion extent. The strongest relationships between behavioral measures and fMRI measures were found for Reach Time ($r = -0.640$, $p = 6.11 \times 10^{-5}$); Reach Distance ($r = -0.538$, $p = 0.001$); Retrieval Distance ($r = -0.481$, $p = 0.005$); Grasp Speed ($r = 0.407$, $p = 0.019$); Retrieval Time ($r = -0.402$, $p = 0.020$); Grasp Time ($r = -0.369$, $p = 0.035$); Reach Speed ($r = 0.361$, $p = 0.039$), with $n = 34$ observations. In agreement with other studies (Chen et al., 2012), the lesser the severity of the lesion, the better the functional recovery and cortical reactivation after lesion. As shown in Fig. 10, differences from pre-lesion fMRI responses demonstrate a tendency for intensive therapy to improve responses to nearly normal between 5 – 8 weeks post-lesion.

### 3.6. Neuronal response properties in affected hand region of area 3b after dorsal column lesions of different extents

We examined neuronal activity using microelectrode mapping to validate the cortical reactivation outcomes indicated by the fMRI activations. To characterize neuronal responsiveness, receptive fields, and somatotopy in affected hand region of area 3b after unilateral DC-lesions, and verify the somatotopy of fMRI activations, multiunit recordings with single or arrays of microelectrodes were made in six monkeys 14–70 weeks after the DC lesion. Multiunit recordings were also made in areas 3a and 1 in order to define the rostrocaudal boundaries of area 3b. However, our main focus was in area 3b. Microelectrode mapping results from the other three monkeys (SM-Hn, SM-Ur, SM-Ya) have been published elsewhere in unrelated studies (Liao et al., 2016; Qi et al., 2019).

**Cases with nearly complete lesions.—**Results were obtained from three cases. (1) In squirrel monkey SM-Fr, an array of 100-microelectrodes was implanted in the hand region of area 3b after a long-term recovery (70 weeks) from an extensive unilateral DC-lesion (91% complete). Neurons in this deprived and recovered region were highly responsive, with only a few unresponsive recording sites. Somatotopically, neurons in many of the mapping sites responded to a touch or taps on the pads of single or multiple digits. Only a few mapping sites were devoted to taps on pads of the palm. Overall, the D2–5 were represented in a roughly lateromedial sequence. However, there was no response to touch on D1 in this monkey (Fig. 11Aa). The neuronal receptive fields were somewhat large for a few

mapping sites in which neurons responded to multiple digits or phalanges. (2) In squirrel monkey SM-Kr, the deprived area 3b was mapped with an array of 100-microelectrodes 26 weeks after an extensive lesion (90% complete) of the contralateral (right) dorsal columns at the C5 level. Again, the vast majority of mapping sites in the hand region of area 3b was responsive, and only a few non-responsive sites were found. However, overall responsiveness was somewhat weaker as compared to those of a normal monkey, with a higher proportion of mapping sites with neurons responding to hard taps (marked with diamonds). The somatotopy of digits 2 – 4 was in a normal lateromedial progression in area 3b. However, no response was found in response to touching digit 1. The neuronal receptive fields in a majority of the mapping sites in area 3b were similar, with only a few mapping sites with neurons that responded to multiple digits or phalanges (Fig. 11Ba). (3) Monkey SM-Ra had an extensive DC-lesion (est. 90% complete) on the right cervical spinal cord level C4-C5 (Supplementary Fig. 1i). The deprived hand region of area 3b was mapped 17 weeks after lesion. An array of 100-microelectrodes was implanted in the deprived hand region of areas 3a and 3b, but the placement was at a more medial location such that the digits 1 and 2 territories were not covered. However, a fair portion of mapping sites in area 3b had neurons that responded to tactile stimulation on digits 3 and 4, and about half of the recorded neurons responded well (Supplementary Fig. 7). As a group, the reactivations of hand cortex was incomplete, with some unresponsive regions, often less responsive regions, and some locations with highly responsive neurons and neuronal receptive fields.

**Cases with large lesions.—**The somatosensory maps in the deprived hand region of area 3b were made at post-lesion 18 weeks for SM-He, 59 weeks for SM-Ur, 19 weeks for SM-Bu, and 14 weeks for SM-Fy (Table 1). The overall results from monkeys in this group indicate that neurons in the deprived hand region of area 3b responded well to touches or taps on affected digits and hand. The RFs sizes from neurons were not abnormally large (except for SM-Ur), as the majority of the receptive field sizes for neurons that respond well were restricted to single digits or palm pad. Representations of digits 1 – 5 were roughly organized in a lateromedial progression, which closely resembled those of normal monkeys (Fig. 11Ca – 11Ea). Squirrel monkey SM-Ur had more mapping sites in area 3b hand region where neurons had large receptive fields and responded to touch or taps on digits, hand, and forelimb combined (see Liao et al., 2016 for a description of the hand region map). It is unclear why SM-Ur differed from other monkeys with intermediate lesion size. The results from this monkey indicated that the hand regions of area 3b and 1 underwent large-scale reorganizations, the neuronal receptive fields were abnormally enlarged, and somatotopy did not reflect a normal pattern.

**Cases with less extensive lesions.—**The comprehensive somatosensory maps from monkeys SM-Ya (65% complete) and SM-Hn (64% complete) in this group have been published elsewhere for other studies (Liao et al., 2016; Qi et al., 2019). The overall findings indicate that extensive DC-lesions at a slightly lower level (C5 – C6) allows most inputs from digit 1 and, likely some from digit 2 to be spared. Final post-lesion electrophysiological mapping was made at 42 weeks in SM-Ya and 20 weeks in SM-He. Cortex representing the spared D1 and D2 in the hand region of areas 3b contralateral to the lesion side were abnormally large at the expense of D3, and possibly D4 territories. Note

that the digits 1 – 4 were somatotopically organized in a lateromedial sequence. The strength of responses to spared D1 and D2 were robust, and somatotopy was comparable to those of normal monkeys. However, neuronal responses recorded from the likely deafferented hand region (i.e., digits 4 – 5, and ulnar palm) were less robust. Neural receptive fields for neurons in this deprived region of area 3b were generally large, involving multiple digits and palm pads.

In summary, after months of recovery from DC-lesions with or without training, neurons in the deprived hand region of area 3b were responsive to touch on hand even in monkeys with extensive lesions. However, the strength of responses were generally weak and receptive field sizes were generally large (involving multiple digits, see next sections) as compared to those monkeys with less extensive lesions.

### 3.7. Quantitative changes in the post-lesion reactivated maps of digits in area 3b

At the end of the recovery periods after DC-lesions, detailed somatosensory maps were acquired from multiple site microelectrode recordings from the area 3b hand region of all nine monkeys in the present study. In each case, part or much of the hand region was reactivated, but did not return to normal. Inspection of the individual maps revealed abnormalities which include unresponsive recording sites where no clear response to touch on the hand was recorded, representation of digits in abnormal locations, and neurons activated by two or more digits or the combination of digit and palm pads. Here we demonstrated that the reactivated area 3b maps consistently differ from normal maps by failing to recapture the full extents of the normal representations of digits, while greatly increasing the proportion of cortex with neurons responsive to multiple digits or digit and palm pads.

In normal squirrel monkeys, individual digits are not represented in territories of equal size. In an early study, Merzenich et al. (1987) mapped the hand region of area 3b in five normal squirrel monkeys with microelectrode and multiunit recordings, as in the present study. Their tabulated results were arranged here and plotted as a bar graph indicating the size of each digit representation as a proportion of the whole hand representation (Fig. 12A). Digits 2 and 3 representations were the largest, followed by digits 1, 4, and 5. However, as digits vary in surface area, and digit 1 has the smallest surface, digit 1 surface had the highest cortical magnification of nearly three times those of digits 3 and 4. In a later report, Jain et al. (1998) found a similar disproportion representation of individual digits in the area 3b hand region of normal owl moneys, with digits 2 and 3 having the largest territories, followed by D1, D4 and D5.

Here, in order to compare sizes of digit representations in area 3b of normal monkeys with those of lesioned monkeys, we measured the areal sizes of digit representations (Fig. 12B) taken from previously published microelectrode maps of area 3b hand cortex from four naïve monkeys (Liao et al., 2013), in which area 3b was mapped with single microelectrode penetrations under the same recording conditions as the maps from DC lesion cases in the present study. The areal sizes from these normal monkeys were similar to those expected based on mapping from decades of research, in which D1, D2, and D3 take up the largest amount of the hand representation (e.g., Merzenich et al., 1987; Jain et al 1998). In the four

naïve squirrel monkeys, the D2 representation was the largest, followed by digits 3, 1, 4 and 5. These results were highly similar, to those reported by Merzenich et al. (1987) and Jain et al. (1998). The slight differences in reported proportions for squirrel monkeys may be related to differences in the estimated sizes of the hand representations, or even differences between squirrel and owl monkeys. However, when these digit representations in normal squirrel monkeys were compared to those with DC-lesions, it became clear that none of the expected territories of the five digits regained their former sizes following a DC-lesion and a recovery and cortical reactivation period of at least 3 months. This failure was partly the result of somatotopic disorganization in the reactivated map so that neurons in roughly 15% of the hand region represented two or more digits or digits and palm pads, while multidigit responses are rare in area 3b of normal monkeys. For detailed proportions of reactivated digit representations in area 3b of each lesioned monkey, see Supplementary Fig. 8.

Another reason why digit representations did not return to normal sizes after recovery from DC-lesions is that all of the area 3b hand region was not reactivated. Thus, neurons at some sites did not respond to touch or even taps on the digits or palm. In normal squirrel monkeys, nearly 100% of recording sites throughout the hand representation encountered neurons that responded to touch (Fig. 12Ca). This value dropped to 80% or less in the nine monkeys studied here after DC-lesions. The results indicate that the somatotopy and neuronal responsiveness in deprived area 3b are highly dependent on the extent and level of DC-lesion. Note that the monkeys with intensive therapy during the recovery period had somewhat greater reactivation of cortex than the minimum therapy monkeys. A related difference between the maps of digits in area 3b of normal squirrel monkeys and the reactivated maps in monkeys with DC-lesions is that all five digits were not always represented in lesioned monkeys (Fig. 12Cb). In normal monkeys, all 5 digits are represented (100%). In monkeys with DC-lesions, the representation of 1 or more digits may be missing, with an average of close to one digit representation missing (80%). Again, note that the representations after DC-lesions and recovery in squirrel monkeys with the behavioral training group were slightly more complete than those of the minimum therapy group. Taken together, the results indicate that the somatotopy and neuronal responsiveness in deprived area 3b is highly dependent on the extent and level of DC-lesion.

### 3.8. Contributions of reactivated digit territories to behavioral recovery

While the expected territories within area 3b for each digit are variably reactivated after recovery from DC-lesions, the reactivations of the territories for digits 1 and 2 are likely to be most important. As shown in Fig. 1B, lesioned monkeys were tested on a Kluver board task in which they attempted to retrieve sugar pellets from wells of increasing depth. As described in Methods session, the monkey initially contacted the food pellet inside of the wells and subsequently pulled out the pellet with digit 2 alone or digits 2 and 3, and secured it against D1 and palm. The thumb was typically flexed throughout the grasp and was therefore not directly involved in handling the food pellet, but helped to secure the pellet during retrieval. We calculated the proportion of each reactivated digit territories in area 3b hand cortex obtained from microelectrode mapping, and correlated those values with the total behavioral recovery rank for each DC-lesion monkey. We found that the amount of cortex reactivated by D1 was best correlated with the total mean rank ($R^2$ = 0.29, Fig.

13A). The amount of cortex for D2 correlated with behavior recovery nearly as well ($R^2$ = 0.21), while the amount of reactivated cortex for D3 did not correlate with total mean rank ($R^2$ = 0.07). The reactivated territories for D4 and D5 also had little or no predictive value. Overall, the combined areal sizes of the reactivated D1 and D2 representations in area 3b, as obtained from microelectrode maps, better correlated with total behavioral outcomes.

Similar trends are apparent in Fig. 13B, in which the magnitudes of the peak signal change of the fMRI responses to vibrotactile stimulation on digits 1 – 3 are compared with total mean rank. The results show that peak magnitudes of fMRI responses to digit 2 stimulation better correlates with behavioral performance ($R^2$ = 0.699) than magnitudes for stimulating on D1 ($R^2$ = 0.195) and D3 ($R^2$ = 0.020). Both results obtained from microelectrode mapping and fMRI mapping indicate that reactivations of digits 1 and 2 territories or fMRI responsiveness best predict behavioral recoveries.

### 3.9. Comparing somatotopies of electrophysiological and fMRI maps

Microelectrode maps of the hand region of New World owl and squirrel monkeys with large numbers of closely spaced electrode penetrations has long been recognized as a standard method of producing highly detailed, reliable, and repeatable maps of the hand representation in both normal monkeys and those that have altered cortical representations due to sensory loss (e.g., Merzenich et al., 1983a; 1983b; Wall et al., 1983). More recently, fMRI maps have proven useful as a non-invasive way of obtaining such maps. Here, we obtained both fMRI and microelectrode maps of the area 3b hand region in the same DC-lesion monkeys, which provided the opportunity to compare the two types of maps. As the post-lesion maps changed over the recovery period, we compared the last fMRI map for each monkey with the terminal microelectrode map. Both maps were obtained late in the recovery period when the maps were likely to be highly stable. For comparison, the two maps were aligned using shared features, sulci and vasculature, and the fMRI images, and the borders of area 3b as determined architectonically, and functionally (see Methods).

The correspondence between fMRI final maps (post-lesion weeks 8 – 12) and electrophysiology maps was high for monkeys with less severely lesions, such as SM-Ya (65% complete) and SM-Hn (64% complete). For SM-Ya, post-lesion week 12 CBV responses for digits 1–3 (circled in red, blue, and yellow in Fig. 11G) overlapped the corresponding microelectrode-defined territories mapped at post-lesion week 42, while the focus of CBV response from digit 4 (circled in green. Fig. 11H) shifted laterally than the corresponding electrophysiological response field. For SM-Hn, the last post-lesion scan (week 8) BOLD activations for digits 1–3 (circled in red, blue, and yellow in Fig. 11H) overlapped the corresponding microelectrode-defined territories mapped at post-lesion week 20. The focus of BOLD response for digit 5 (circled in purple) shifted laterocaudally as compared to the corresponding electrophysiological response territories. Congruence between the two maps, however, was poorer in the monkeys with most severe lesions. For SM-Fr (91% complete), there was roughly lateromedial somatotopy of digits 1, 3, 4, and 5 in the 8-week fMRI map (circles in Fig. 11Ab), the same was true for digits 2–5 in the microelectrode map at post-lesion week 70 (shades in Fig. 11Ab). However, there was little overlap between these two maps except for the location of digit 5 (purple circle and shading

in Fig. 11Ab). Similarly, in another severely lesioned monkey SM-Kr (90% complete), the last BOLD map (week 9) revealed responsive foci from vibrotactile stimulations on digits 1, 3, and 5 (circled in red, yellow and purple in Fig. 11Bb), which were arranged in lateromedial somatotopy. In comparison, the microelectrode map at post-lesion week 26 revealed neurons in area 3b which responded well to tactile stimulation on digits 2, 3, and 4, and they were arranged in a lateromedial progression pattern as in that of normal monkey (shades in Fig. 11Bb). However, there was no overlap between BOLD map and microelectrode map (Fig. 11Bb). For the other four monkeys who had intermediate extent of lesions, partial overlaps between the two maps were present (Fig. 11Cb – 11Fb). In Qi et al. 2016b, the two types of maps showed better congruence in cases with less extensive lesions and shorter delays between fMRI and microelectrode mapping (Figs. 11 - 15). The present results of incongruent activation maps may indicate co-registration errors in cases with the most extensive lesions. Another likely contributor may be lower signal to noise ratio (SNR) of fMRI signals of the input deprived cortex compared to the relatively higher SNR of neuronal spiking activity from the microelectrode maps.

## 4. Discussion

The present results come from a total of nine monkeys that have been extensively studied after unilateral lesions of primary afferents from the hand as they course in the dorsal columns to terminate in the cuneate nucleus of the upper spinal cord and adjoining brainstem. Our interest in this dorsal column lesion model of sensory loss stems from its usefulness in depriving higher order somatosensory structures of their activating inputs without notably impairing overall behavior. The unilateral lesions in the cervical spinal cord immediately deactivate most or all of the representation of the hand in contralateral area 3b, as well as the hand representations in higher cortical areas, the ventroposterior nucleus, and ipsilateral cuneate nucleus. The use of the ipsilateral hand is impaired in reaching and retrieving small objects, and the monkeys act as if they do not feel light touch on the hand. Yet, they use this forelimb to run and climb as in intact monkeys. Remarkably, skilled hand use and a considerable reactivation of hand representation in contralateral cortex by afferents from the hand return over weeks to months of recovery. This recovery appears to depend on a small number of preserved dorsal column afferents from the hand, and a number of secondary inputs from dorsal horn neurons with somatosensory inputs (Liao et al., 2018; Qi et al., 2019). Here we addressed several important issues about the recovery patterns and their relation to variables in lesion size and effectiveness, sensory experience, and measures of cortical reactivation. To reveal relationships, we quantified variables in DC-lesions, reaching and retrieval behavior, and the restoration of cortical hand representations. We evaluated the use of fMRI to chart the time course of the reactivation of the cortical map of the hand, compared BOLD and CBV signals in fMRI, and related fMRI maps to those obtained by microelectrode mapping methods. We compared cortical reactivation and behavioral recoveries in monkeys with extensive post-lesion training on our reach and retrieval task with monkeys with only weekly testing. Here we discuss our main results, and the methods to obtain these results.

There are four main findings. (**1**) Results from a large group of monkeys confirm previous findings that damage to dorsal column afferents from the hand initially impairs hand use

and reduces or eliminates the activity evoked in contralateral hand cortex by touch on the hand. The BOLD or CBV fMRI responses in cortex and skilled use of the deprived hand largely recovered over weeks to months. Small numbers of spared dorsal column axons are critical to the reactivation and recovered behavior. (**2**) Intensive therapy of the impaired hand tends to promote early behavioral recovery and early cortical reactivation as determined with longitudinal fMRI. (**3**) Even in cases with nearly complete lesions, the deprived region of contralateral area 3b was mostly responsive to touch on the hand after months of recovery. On average, neurons in deprived cortex had a slightly greater proportion of responsive neurons in the intensive therapy group than the minimum therapy group. Where the microelectrode recordings were most useful in revealing the nature of reactivated cortex, BOLD and CBV fMRI responses revealed reactivations. (**4**) When the reactivation of cortex for each of the digits was considered, the reactivation by digit 2 stimulation as measured with microelectrode maps and fMRI maps was the best correlated with overall behavioral recovery, corresponding to use of digit 2 to perform the retrieval task by these monkeys.

### 4.1. Quantitative comparisons of the completeness of the lesions, cortical reactivations, and behavioral recoveries

**Spinal cord lesions.—**Estimates of the completeness of spinal cord lesion can be difficult to judge by a reconstruction of the lesion site alone, in part because adjacent parts of the spinal cord tend to migrate into the lesion zone and the histological sectioning can introduce tears in fragile tissue. For injuries of the dorsal columns, our estimates of lesion effectiveness have been quantified by directly labeling dorsal column axons from three digits from the lesioned side and the intact side and comparing the two sets of terminations in the cuneate nucleus. The proportional reduction of labeled axons from the lesioned side is then used to represent the percent loss for all digits or the whole hand. The relative locations of terminal paths of labeled axons can be used to identify the digits of their origin. The labeled regions in the dorsal horn relative to the lesion site help identify the cervical level of the lesion as well as the spared inputs that enter the spinal cord above the lesion (Qi et al., 2011). We injected tracer into digits 1, 3, and 5 to cover the range of digit inputs, but given the importance of preserved inputs from especially digit 1 and 2, and perhaps 3 in behavioral recoveries of hand use, it may be more relevant to label inputs from digits 1 –3 in future studies. If distinguishable tracers can be used, it may be possible to label inputs from all digits and parts of the palm for a more complete assessment. In addition, if fMRI is used to detect reactivation from specific digits in area 3b in experimental monkeys or humans with spinal cord injury, early post-lesion responses in hand cortex during the stimulation of digits 1 and 2 would best predict the recovery of normal hand use (see below).

**Cortical reactivation.—**The somatotopy of the reactivated map of the hand in monkeys after sensory loss has been traditionally accessed by microelectrode recordings of receptive field locations from neurons at a large number of sites across the area 3b hand region. As these maps can be reconstructed in great detail, and such maps are very stable in normal and experimental monkeys (Wall et al., 1983; Merzenich et al., 1983a; 1987; Sur et al., 1982; Pons et al., 1987), microelectrode maps have been considered to be the gold standard for determinations of map organization. In support of this premise, microelectrode

maps of the digit representations compare well with those based on histological criteria (Jain et al., 1998). As fMRI maps of the hand representation can be done in monkeys at high resolution (Chen et al., 2007; Zhang et al., 2010), and such maps have been used to chart the recovery process of somatosensory cortex after dorsal column lesion in experiments with repeated imaging sessions (Chen et al., 2012; Dutta et al., 2014; Yang et al., 2014; Qi and Wang et al., 2016a; Wu et al., 2017). As in the present study, fMRI maps can also be done with microelectrode recordings (Wall et al., 1983; Merzenich et al., 1983b) or with implanted microelectrode arrays (Jain et al., 2001; Qi et al., 2016b), but with clear drawbacks. Our fMRI results on the detectability of cortical activations in area 3b hand cortex while stimulating digits on the impaired hand indicate that both BOLD and CBV signals are similar and useful, although CBV imaging with MION produced larger peak response magnitudes across all pre- and post-lesion imaging responses in our study. However, dorsal column lesions produced proportionally similar reductions in peak magnitudes of both signals. As expected, dorsal column lesions had great impact within the first few post-lesion weeks, most notably for the nearly complete lesions. Over longer recovery times, part of the hand representation in area 3b became reactivated, but with alterations in somatotopy. Comparisons with terminal microelectrode maps were most similar when the fMRI maps were from cases with less complete lesions, or after longer recovery times. FMRI responses to the most deprived digits were variable in magnitude (examined quantitatively) and location (assessed qualitatively) over time. The mis-located activations may reflect the formation of abnormal connections, but the evidence for this is limited and requires further study.

**Behavioral recoveries.—**The advantages of using the reach-to-grasp task as a model to study training effects on impairment and subsequent recovery from DC-lesions are four-fold: (1) The reach-to-grasp task is widely used in stroke and spinal cord injury among a variety of animal models including rodents (Ballermann et al., 2001; Krajacic et al., 2010; Starkey and Schwab, 2012; Wahl et al., 2014;) non-human primates and humans (e.g., Nudo et al., 1996a, b; Darian-Smith and Ciferri, 2005; Fisher et al., 2020; Nishimura et al., 2007, 2009; Murata et al., 2008; Rosenzweig et al., 2010; Nout et al., 2012a,b; Friedli et al., 2015; Zaaimi et al., 2012). By using four distinct, complementary, and sophisticated reach and grasp tasks for macaque monkeys, Schmidlin et al. (2011) showed how the behavioral data can be exploited to investigate the impact of a spinal cord lesion and to what extent a treatment may enhance the spontaneous functional recovery. Using a similar but simpler reach-to-grasp task allowed us to compare our results with those obtained from other studies; (2) Current results can be compared with our earlier results collected from minimum therapy squirrel monkeys after a DC-lesion (Qi et al., 2013; Qi and Reed et al., 2014). Previous studies with squirrel monkeys show that although hand function of monkeys is severely impaired after extensive DC-lesions, considerable hand function recovers over time. (3) Kinematic analyses of reach-to-grasp actions suggest that the underlying cortical circuits in non-human primates are organized in a similar manner as in humans (see Karl and Whishaw, 2013; Flindall and Gonsalez, 2019 for review). (4) Reaching to grasp food is a natural and routine habit of monkeys in daily life that therefore requires very little training.

We have previously detected impairments in a reach and retrieval of a food pellets task using a modified Kluver Board (Kluver, 1935), and were able to track the course of behavior recovery with the recovery of cortical activation (Qi et al., 2013), as in the present study. As the behavior has been video recorded, aspects of the behavior can be measured and scored, and related to other variables such as recovery time, lesion size, cortical reactivation, and behavioral training. The measured behaviors included not only success scores and numbers of attempts at pellet retrieval, but also on the trajectories and speeds of reach, grasp and retrieval movements. These measures allowed a fuller understanding of the cortical recovery process. Most notably, the post-lesion hand trajectories were less direct in relation to the target (also see Qi et al., 2013). This behavioral change appeared in part to reflect a compensation for a lack of ability to use touch to determine if the food pellet was safely in the grasp of the deprived hand. Thus, the monkeys became more dependent on vision, and they rotated their hand to see if the pellet was in the hand; thus, taking longer to reach and retrieve. These additional quantitative measures, in addition to success scores, allowed more aspects of the behavior to be related to the completeness of the dorsal column lesions, the reactivation of cortex, and the extensive intensive therapy. Over post-lesion recovery time, behaviors returned toward normal, suggesting the gradual return of tactile sensations on the hand.

### 4.2. Effects of lesion on behavioral recovery

Our present results are consistent with previous findings that the more complete the dorsal column lesion, the more the behavior is impaired and the longer it takes for behavioral recovery (Qi et al., 2013). Moreover, our fMRI and electrophysiological results now provide additional evidence that recovery of task-specific dexterity is highly dependent on the direct primary afferents from the hand which are spared at the level of individual digit afferents. In the pellet retrieval task, the afferents from digit 2 seemed to contribute most to recovery of task performance, as digit 2 is the most used in grasping small objects. Inputs from other digits are less critical, as are inputs from the palm. Large lesions not only remove nearly all of the primary afferents, but also many of secondary afferents that carry somatosensory information to the cuneate nucleus (Liao et al., 2018). In addition, the most complete lesions greatly reduce the competition for synaptic space that normally occurs in cuneate nucleus so that the formation of abnormal connections within the nucleus may provide misleading and confusing information that could impact behavior. Extensive behavioral training could activate and strengthen preserved neural circuits over new and potentially maladaptive circuits. Here we attempted to determine if moderate amounts of task specific behavioral therapy could improve recovery, and if such improvements related to the extent of lesion, and the fMRI map of somatosensory area 3b. We found that the extent of the DC-lesion was highly correlated with the behavioral outcome. Additionally, task-specific training promotes earlier cortical reactivation and specific aspects of behavioral recovery. Our statistical comparisons indicate that the proportion of axon sparing from the lesion is the most important factor in the functional recovery.

However, secondary neurons in the dorsal horn of the spinal cord that are activated by branches of cut primary dorsal column axons could play a role in the cortical reactivation and behavioral recovery, but the role of these remaining inputs in the recovery process has

not been studied. More likely, behavioral compensations play a role, as macaque monkeys with no sensory input from the hand can learn with extensive training to reach and retrieve objects (see Taub, 2014, Taub et al., 2002, 2014 for review). While our monkeys sometimes used vision to see if unfelt sugar pellets were in the grasp of the deprived hand, they did not continue this practice after recovery times that apparently allowed them to feel the touched pellets (Qi et al., 2011). We did have cases where no axon terminals from the injected digits were labeled in the cuneate nucleus, suggesting a 100% complete lesion. These monkeys had no cortical reactivations by these digits, and have limited behavioral recoveries (Liao et al., 2016, 2018, Qi et al., 2019). Secondary pathways may have played role in the limited recoveries.

As some DC lesions encroached into descending motor pathways and the gray matter of the spinal cord, it seems unlikely that such additional damage would affect the microelectrode mapping or the fMRI activation results. However, the involvement of motor pathways could impact reaching and grasping skills in monkeys (Sasaki et al., 2004; Schmidlin et al., 2004; Murata et al., 2008; Nishimura et al., 2007, 2009; Rosenzweig et al., 2010; Kinoshita et al., 2012; Nout et al., 2012a,b; Zaaimi et al., 2012; Friedli et al., 2015), but not the recovery of touch, which is essential for grasping and retrieving pellets without visual guidance. As mentioned elsewhere, monkeys appeared to use vision to see if the grasp held the pellet early in recovery periods (e.g., Qi et al., 2011). It would be useful to evaluate the reach and retrieval behavioral when vision is blocked.

### 4.3. Effects of task-specific training on functional recovery after DC-lesion

Large bodies of evidence indicate that behavioral experience and activity-dependent plasticity are important drivers in functional recovery after injuries, including cut nerves (e.g., Florence et al., 1998, 2001), stroke (e.g., Nudo et al., 1996a; Xerri et al., 1996; Edwards et al., 2019; see Wahl and Schwab, 2014, Dobkin 2008 for review), dorsal rhizotomy (Darian-Smith and Ciferri 2005), and SCI (see Buonomano and Merzenich 1998; Jones 2000; Tetzlaff et al., 2009; Kleim, 2011; Fouad and Tetzlaff, 2012; Sofroniew 2018 for review). Further, the clinical outcome after stroke can be markedly improved by sensory rehabilitation (Kunkel et al., 1999; Kopp et al., 1999; see Taub et al., 2002; Allred et al., 2014 for review).

In the present study, the therapy procedure was started on the post-lesion day five with the repetition of five days a week for monkeys in the intensive therapy group. Generally, most of monkeys initially switched hands and tried to use the preferred (intact) hand to retrieve pellets after lesion. In order to encourage monkeys to re-learn to use the impaired hand, we used a few strategies to prevent use of the intact hand by setting up the window aperture in such way that it would be difficult for the monkey to retrieve pellets with the intact hand; blocking or covering the pellets when they tried to reach with the intact hand; or gently holding their intact hand when it was possible during reach-to-grasp trials. For minimum therapy monkeys, we also used the same strategies to encourage them to use impaired hands on the testing day (1 – 2 times per week for fewer trials, see Methods), however, we would stop testing if they continued to only use their intact hands. As a result, we found that most of the monkeys with intensive therapy were able to use their impaired

hands to perform reach-to-grasp task within the first few weeks after lesion. In contrast, it took longer time for minimum therapy monkeys to retrieve food items even when the lesion was less extensive (e.g., SM-Bu). Such longer times for recovery were also found and briefly described in another study with minimum therapy monkeys (Qi et al., 2019). These findings suggest that early rehabilitative intervention is effective in accelerating behavioral recovery after injury. This result is in agreement with Taub's studies using Constraint Induced (CI) therapy after brain damage such as traumatic brain injury, cerebral palsy, multiple sclerosis, stroke, and spinal cord injury in patients (see Taub et al., 2002; Taub, 2014; Taub et al., 2014 for review). The CI therapy is thought to strengthen diminished neural connections with use-dependent plasticity.

Studies have shown that intensive behavioral therapy improves not only behavioral recovery but also structural and functional reorganization in the central nervous system. For instance, Nudo and colleagues (1996a) reported that intensive behavioral therapy of naïve adult squirrel monkeys in a digits-skill task resulted in primary motor cortex (M1) reorganization by increasing the amount of cortex dedicated to the specific movements and movement combinations important for the motor skill. After damage to a portion of the hand representation in M1 of adult squirrel monkeys without rehabilitative training, a further loss of hand territory in the adjacent, undamaged cortex was found. However, in monkeys that underwent rehabilitative training with the impaired limb after similar infarcts resulted in preserving and expanding of hand territory in cortex adjacent to the infarct (Nudo et al., 1996b). This functional reorganization in the undamaged motor cortex was accompanied by behavioral recovery of skillful use of the hand function. Based on the quantity and quality of motor experience, Nudo surmised that the brain can be reshaped after injury in either adaptive or maladaptive ways, and suggested that behavioral experience is the most potent modulator of brain plasticity (see Nudo, 2013 for review).

Here we presented findings that suggest use dependent activities in area 3b may help restore normal-like somatotopy and limit the abnormalities after sensory loss. After long-term recoveries (more than 5 months) from extensive DC-lesions, neurons in parts of the deprived hand region of area 3b sometimes represented inputs from other parts of the body. Thus, in a minimum therapy monkey with a 90% complete DC-lesion, neurons in the digit 2 territory of area 3b responded to touch or taps on the face or both the hands and the face. Face responsive neurons were found as far as 2 mm or more from the normal hand-face border (Supplementary Fig. 7). However, neurons responsive to the face were not found within the hand region of area 3b in intensively trained monkeys (SM-Fr and SM-Kr) with extensive DC-lesions (91% and 90% complete, respectively) and long recovery times. In a third monkey (SM-Ur, 86% complete) with an extensive DC-lesion and an extra-long recovery period (414 days), and with post-lesion intensive task specific therapy of hand use, again no face responsive neurons were found in the deprived hand region of area 3b (see Liao et al., 2016 for a description of the hand region map). Nevertheless, nearly half of the mapping sites had neurons with abnormally large or mislocated receptive fields on multiple digits, other parts of the hand, and even the forearm. These results suggest that training, recovery time, or both contribute to reorganization of hand cortex in area 3b. Taken together, these findings suggest that use- or activity-dependent plasticity drives normal somatotopy and prevents maladaptive alternatives after area 3b deafferentation.

When correlated with behavioral outcome, we found that in monkeys with incomplete DC-lesions and intensive therapy, primary somatosensory areas underwent large-scale reorganization, such that spared inputs from the digits, hand, and forelimb expanded into deprived hand territories; and the responsiveness of cortical neurons to touch or taps on hand and forelimb was higher than that of monkeys without intensive therapy. Overall, these changes in neural reactivation in the deprived cortex were associated with behavioral recovery of hand use in a reach-to-grasp task. However, if the lesion was nearly complete, training was not effective in improving cortical somatotopy and responsiveness. The persistent functional deficits are most likely due to a more complete loss of primary and secondary sensory inputs to the cuneate nucleus from the hand.

We speculate that adjustments of the training paradigm may result in further improvement in the recovery process. In patients with incomplete spinal cord injury, there is evidence that repetitive and intensive practice can induce practice-dependent brain and spinal plasticity, and that exercise intensity has a profound effect on sensorimotor recovery (Dietz et al., 2002; Beekhuizen and Field-Fote, 2005). However, while such repetitive training could facilitate use-dependent mechanisms of synaptic selection, and produce a powerful influence on somatosensory cortical organization and recovery of behavioral performance (Merzenich et al., 1996), it is difficult to effectively increase the training frequency and intensity for the best results in our current experimental paradigms. Thus, other interventions that passively but efficiently excite the injured pathway could be used to strengthen the specific rewiring.

### 4.4. Statistical comparison of relationship

The three lesion extent categories used in statistical modeling significantly predicted the difference in mean fMRI responses as the largest main effect, along with the time period post-lesion. The training condition had a weaker but significant main effect. The task-specific intensive therapy tended to provide benefit for earlier improvement in aspects of dexterity and corresponding cortical recovery, even when the lesion was extensive. Note that all cases improved if the injury was incomplete. The largest difference, however, was at the post-2 time period, indicating the tendency of cases with training to improve fMRI signal changes closer to pre-lesion levels in the period of week 5–8. Across cases, we found fMRI responses from spared digits could be detected as early as week 2 post-lesion. However, fMRI responses to stimulation of the most deprived D3 – D5 were varied in the hand region in area 3b over post-lesion weeks.

Spinal cord injuries in patients are variable and a proper diagnosis is a crucial step for planning appropriate therapeutic strategies and treatments. Non-invasive and longitudinal evaluations of behavioral impairment and cortical response after injury serve this purpose well. Statistical modeling can be used to detect variables with the closest correlations among factors such as extent of lesion, behavioral measurements, and/or cortical reactivations. Further, access to fMRI responses can provide distinct information about the level of sparing that is not provided by certain types of behavioral testing. Our results suggest that certain behavioral measurements such as the number of attempts to retrieve pellets from the most difficult task (i.e., Well 4), and performance time were correlated better to cortical reactivation than other behavioral measurements (e.g., success and distance) in the current

testing model. Collectively, all of these measures are particularly good predictors of brain recovery when the extent of the lesion is unknown. Intensive therapy may result in faster recovery, but with incomplete lesions and long recovery periods, similar levels of recovery may be possible without behavioral training. If the injury is extensive, little recovery occurs without additional interventions. Although our results indicate that the recovery of skillful hand use is highly dependent on preserved primary axon inputs from digits, inputs from digit 1 in human and macaques may be more important in tasks requiring precision grip (Baldwin et al., 2018).

### 4.5. BOLD MRI vs. CBV MRI

In the present study, we obtained measures of the post-lesion reactivation of primary somatosensory cortex before and after DC-lesion using two types of fMRI responses: blood oxygen level dependent (BOLD) and cerebral blood volume (CBV). The post-lesion images were compared to pre-lesion images for each monkey. Note that CBV measures of evoked activity use a intravascular contrast agent of monocrystalline iron oxide nanoparticles (MION) to increase the sensitivity in detecting blood volume changes (Mandeville et al., 1998; Kennan et al., 1998; Vanduffel et al., 2001; Kim et al., 2013). The contrast to noise ratio (CNR) of CBV-weighted fMRI depends primarily upon the percent change in blood volume, while the CNR of BOLD fMRI depends upon the absolute change in deoxygenated hemoglobin level. The magnitude of CNR with CBV is larger relative to BOLD imaging (Mandeville et al., 1998, 2001; Kennan et al., 1998). The common understanding is that CBV and BOLD responses do not completely overlap because BOLD signal is biased toward large draining veins while CBV is more spatially constrained and aligned closely to the neural activity (e.g., Fukuda et al., 2006; Kennerley et al., 2010). By comparing spatial specificity between BOLD and CBV imaging at 4.7T in the visual cortex of anesthetized macaques, Smirnakis et al. (2007) found that visually driven CBV modulation is relatively stronger in deep versus superficial cortical layers compared with the BOLD modulation. However, under large surround stimulation conditions, CBV modulation covered a larger cortical area than BOLD, leading the group to conclude that ‘the spatial profiles of BOLD and CBV activity maps do not co-register across all stimulus conditions, and therefore do not necessarily represent equivalent transforms of the neural response”.

In our study, both BOLD and CBV activations were obtained under the same data acquisitions and vibrotactile stimulation conditions with high-resolution 9.4T. The responding foci roughly overlapped with more precise electrophysiological maps for both BOLD and CBV signals, especially when the lesion was less extensive, in agreement with earlier studies (Chen et al., 2012; Wu et al., 2016, 2017; Qi and Wang et al., 2016a). Here, we focused on the comparisons of pre- and post-lesion fMRI responses for each monkey, and both BOLD and CBV maps provided valuable information on spatiotemporal trajectory of cortical plasticity after the DC-lesion.

## 5. Summary and conclusions

Extensive damage to the dorsal column in the cervical spinal cord deactivated the contralateral somatosensory hand cortex and impaired hand use in a pellet retrieval task

in squirrel monkeys. Considerable cortical reactivation and behavioral recovery occurred over the following weeks to months post-lesion. Task specific training of the impaired hand tended to promote an earlier behavioral recovery and an earlier cortical reactivation. Specific kinematic measures of hand movements in the select retrieval task predicted recovery time and related to lesion characteristics better than overall task performance success. CBV fMRI may detect lower levels of cortical activation after injury compared to BOLD fMRI. When the reactivation of cortex for each of the digits was considered, the reactivation by digit 2 stimulation as measured with microelectrode maps and fMRI maps was the best predictor of the overall behavioral recovery. The lesion extent as estimated by preserved primary inputs from the digits to the cuneate nucleus was the key factor in functional recoveries after dorsal column lesions.

## Supplementary Material

Refer to Web version on PubMed Central for supplementary material.

## Acknowledgements

We thank Laura Trice for excellent technical support, and Mary Feurtado for assistance in animal surgery and care; Drs. Chia-Chi Liao, Omar A. Gharbawie, Denis Matrov, Barbara Jones, Christina Cerkevich, Daniel Miller for data collection; Chaohui Tang and Fuxue Xin for assistance in fMRI data collection. This research was supported by National Institute of Health [NS16446] to JHK, [NS067017] to HXQ, [314739] Craig H. Neilsen Foundation fellowship to JLR and JHK.

## Data and code availability statements

The authors confirm that the data for behavioral and statistical analysis within this article will be made available following reasonable requests to Authors. That includes Excel files of numerical data used to generate Fig 2C-D, Fig 3, Fig 4, Fig 5, Fig 9, Fig 10, Fig 12, Fig 13, SI Fig 2, SI Fig 3, and SI Fig 7.

## References

Allred RP, Kim SY, Jones TA, 2014. Use it and/or lose it-experience effects on brain remodeling across time after stroke.Front. Hum. Neurosci8, 379. [PubMed: 25018715]

Andrews SC, Curtin D, Hawi Z, Wongtrakun J, Stout JC, Coxon JP, 2020. Intensity matters: high-intensity interval exercise enhances motor cortex plasticity more than moderate exercise.Cereb Cortex30, 101–112. [PubMed: 31041988]

Baldwin MKL, Cooke DF, Goldring AB, Krubitzer L, 2018. Representations of fine digit movements in posterior and anterior parietal cortex revealed using long-train intracortical microstimulation in macaque monkeys.Cerebral Cortex (New York, N Y: 1991)28, 4244–4263.

Ballermann M, McKenna J, Whishaw IQ, 2001. A grasp-related deficit in tactile discrimination following dorsal column lesion in the rat.Brain Res. Bull54, 237–242. [PubMed: 11275414]

Beekhuizen KS, Field-Fote EC, 2005. Massed practice versus massed practice with stimulation: effects on upper extremity function and cortical plasticity in individuals with incomplete cervical spinal cord injury.Neurorehabil. Neural. Repair19, 33–45. [PubMed: 15673842]

Buonomano DV, Merzenich MM, 1998. Cortical plasticity: from synapses to maps.Annu. Rev. Neurosci21, 149–186. [PubMed: 9530495]

Burns AS, Marino RJ, Kalsi-Ryan S, Middleton JW, Tetreault LA, et al., 2017. Type and Timing of rehabilitation following acute and subacute spinal cord injury: a systematic review.Global Spine J7, 175S–194S. [PubMed: 29164023]

Chen LM, Qi HX, Kaas JH, 2012. Dynamic reorganization of digit representations in somatosensory cortex of nonhuman primates after spinal cord injury.J. Neurosci32, 14649–14663. [PubMed: 23077051]

Chen LM, Turner GH, Friedman RM, Zhang N, Gore JC, et al., 2007. High-resolution maps of real and illusory tactile activation in primary somatosensory cortex in individual monkeys with functional magnetic resonance imaging and optical imaging.J. Neurosci27, 9181–9191. [PubMed: 17715354]

Corniani G, Saal HP, 2020. Tactile innervation densities across the whole body.J. Neurophysiol124, 1229–1240. [PubMed: 32965159]

Darian-Smith C, Ciferri MM, 2005. Loss and recovery of voluntary hand movements in the macaque following a cervical dorsal rhizotomy.J. Comp Neurol491, 27–45. [PubMed: 16127695]

Darian-Smith C, Fisher K, 2019. Somatosensory system organization in mammals and response to spinal injury.Oxford Research Encyclope-dia of NeuroscienceOxford universitu Press, Oxford, UK.

Dietz V, 2016. Improving outcome of sensorimotor functions after traumatic spinal cord injury.F1000Res5.

Dietz V, Fouad K, 2014. Restoration of sensorimotor functions after spinal cord injury.Brain137, 654–667. [PubMed: 24103913]

Dietz V, Muller R, Colombo G, 2002. Locomotor activity in spinal man: significance of afferent input from joint and load receptors.Brain125, 2626–2634. [PubMed: 12429590]

Dobkin BH, 2008. Training and exercise to drive poststroke recovery.Nat. Clin. Pract. Neurol4, 76–85. [PubMed: 18256679]

Dutta A, Kambi N, Raghunathan P, Khushu S, Jain N, 2014. Large-scale reorganization of the somatosensory cortex of adult macaque monkeys revealed by fMRI.Brain Struct. Function219, 1305–1320.

Edwards LL, King EM, Buetefisch CM, Borich MR, 2019. Putting the “Sensory” into sensorimotor control: the role of sensorimotor integration in goal-directed hand movements after stroke.Front. Integr. Neurosci13, 16. [PubMed: 31191265]

Fisher KM, Garner JP, Darian-Smith C, 2020. Reorganization of the primate dorsal horn in response to a deafferentation lesion affecting hand function.J. Neurosci40, 1625–1639. [PubMed: 31959698]

Flindall J, Gonzalez CLR, 2019. On the Neurocircuitry of Grasping: the influence of action intent on kinematic asymmetries in reach-to-grasp actions.Atten. Percept Psychophys81, 2217–2236. [PubMed: 31290131]

Florence SL, Boydston LA, Hackett TA, Lachoff HT, Strata F, Niblock MM, 2001. Sensory enrichment after peripheral nerve injury restores cortical, not thalamic, receptive field organization.Eur. J. Neurosci13, 1755–1766. [PubMed: 11359527]

Florence SL, Taub HB, Kaas JH, 1998. Large-scale sprouting of cortical connections after peripheral injury in adult macaque monkeys.Science282, 1117–1121. [PubMed: 9804549]

Fouad K, Tetzlaff W, 2012. Rehabilitative training and plasticity following spinal cord injury.Exp. Neurol235, 91–99. [PubMed: 21333646]

Friedli L, Rosenzweig ES, Barraud Q, Schubert M, Dominici N, et al., 2015. Pronounced species divergence in corticospinal tract reorganization and functional recovery after lateralized spinal cord injury favors primates.Sci. Transl. Med7, 302ra134.

Fukuda M, Moon C-H, Wang P, Kim S-G, 2006. Mapping iso-orientation columns by contrast agent-enhanced functional magnetic resonance imaging: reproducibility, specificity, and evaluation by optical imaging of intrinsic signal.J. Neurosci26, 11821–11832. [PubMed: 17108155]

Gallyas F, 1979. Silver staining of myelin by means of physical development.Neurol. Res1, 203–209. [PubMed: 95356]

Gharbawie OA, Stepniewska I, Kaas JH, 2011. Cortical connections of functional zones in posterior parietal cortex and frontal cortex motor regions in new world monkeys.Cereb Cortex21, 1981–2002. [PubMed: 21263034]

Jain N, Catania KC, Kaas JH, 1997. Deactivation and reactivation of somatosensory cortex after dorsal spinal cord injury.Nature386, 495–498. [PubMed: 9087408]

Jain N, Catania KC, Kaas JH, 1998. A histologically visible representation of the fingers and palm in primate area 3b and its immutability following long-term deafferentations.Cerebral. Cortex (New York, N Y: 1991)8, 227–236.

Jain N, Qi HX, Collins CE, Kaas JH, 2008. Large-scale reorganization in the somatosensory cortex and thalamus after sensory loss in macaque monkeys.J. Neurosci28, 11042–11060. [PubMed: 18945912]

Jain N, Qi HX, Kaas JH, 2001. Long-term chronic multichannel recordings from sensorimotor cortex and thalamus of primates.Prog. Brain Res130, 64–72. [PubMed: 11480289]

Jones EG, 2000. Cortical and subcortical contributions to activity-dependent plasticity in primate somatosensory cortex.Annu. Rev. Neurosci23, 1–37. [PubMed: 10845057]

Karl JM, Whishaw IQ, 2013. Different evolutionary origins for the reach and the grasp: an explanation for dual visuomotor channels in primate parietofrontal cortex.Front. Neurol4, 208. [PubMed: 24391626]

Kennan RP, Scanley BE, Innis RB, Gore JC, 1998. Physiological basis for BOLD MR signal changes due to neuronal stimulation: separation of blood volume and magnetic susceptibility effects.Magn. Reson. Med40, 840–846. [PubMed: 9840828]

Kennerley AJ, Mayhew JE, Redgrave P, Berwick J, 2010. Vascular origins of BOLD and CBV fMRI signals: statistical mapping and histological sections compared.Open Neuroimag J4, 1–8. [PubMed: 20563253]

Kim SG, Harel N, Jin T, Kim T, Lee P, Zhao F, 2013. Cerebral blood volume MRI with intravascular superparamagnetic iron oxide nanoparticles.NMR Biomed26, 949–962. [PubMed: 23208650]

Kinoshita M, Matsui R, Kato S, Hasegawa T, Kasahara H, et al., 2012. Genetic dissection of the circuit for hand dexterity in primates.Nature487, 235–238. [PubMed: 22722837]

Kleim JA, 2011. Neural plasticity and neurorehabilitation: teaching the new brain old tricks.J Commun Disord44, 521–528. [PubMed: 21600589]

Kluver H, 1935. An auto-multi-stimulation reaction board for use with sub-human primates.J. Psychol1, 123–127.

Kopp B, Kunkel A, Muhlnickel W, Villringer K, Taub E, Flor H, 1999. Plasticity in the motor system related to therapy-induced improvement of movement after stroke.Neuroreport10, 807–810. [PubMed: 10208552]

Krajacic A, Weishaupt N, Girgis J, Tetzlaff W, Fouad K, 2010. Training-induced plasticity in rats with cervical spinal cord injury: effects and side effects.Behav. Brain Res214, 323–331. [PubMed: 20573587]

Kunkel A, Kopp B, Muller G, Villringer K, Villringer A, et al., 1999. Constraint-induced movement therapy for motor recovery in chronic stroke patients.Arch. Phys. Med. Rehabil80, 624–628. [PubMed: 10378486]

Liao C-C, Gharbawie OA, Qi H, Kaas JH, 2013. Cortical connections to single digit representations in area 3b of somatosensory cortex in squirrel monkeys and prosimian galagos.The J. Comparative Neurol521, 3768–3790.

Liao C-C, Reed JL, Qi H-X, Sawyer EK, Kaas JH, 2018. Second-order spinal cord pathway contributes to cortical responses after long recoveries from dorsal column injury in squirrel monkeys.Proc. Natl. Acad. Sci. United States America115, 4258–4263.

Liao CC, Reed JL, Kaas JH, Qi HX, 2016. Intracortical connections are altered after long-standing deprivation of dorsal column inputs in the hand region of area 3b in squirrel monkeys.J. Comp. Neurol.

Mandeville JB, Jenkins BG, Kosofsky BE, Moskowitz MA, Rosen BR, Marota JJ, 2001. Regional sensitivity and coupling of BOLD and CBV changes during stimulation of rat brain.Magnetic Resonance Med45, 443–447.

Mandeville JB, Marota JJ, Kosofsky BE, Keltner JR, Weissleder R, et al., 1998. Dynamic functional imaging of relative cerebral blood volume during rat forepaw stimulation.Magn. Reson. Med39, 615–624. [PubMed: 9543424]

Merzenich MM, Jenkins WM, Johnston P, Schreiner C, Miller SL, Tallal P, 1996. Temporal processing deficits of language-learning impaired children ameliorated by training.Science271, 77–81. [PubMed: 8539603]

Merzenich MM, Kaas JH, Sur M, Lin CS, 1978. Double representation of the body surface within cytoarchitectonic areas 3b and 1 in “SI” in the owl monkey (Aotus trivirgatus).J. Comp. Neurol181, 41–73. [PubMed: 98537]

Merzenich MM, Kaas JH, Wall J, Nelson RJ, Sur M, Felleman D, 1983a. Topo-graphic reorganization of somatosensory cortical areas 3b and 1 in adult monkeys following restricted deafferentation.Neuroscience8, 33–55. [PubMed: 6835522]

Merzenich MM, Kaas JH, Wall JT, Sur M, Nelson RJ, Felleman DJ, 1983b. Progression of change following median nerve section in the cortical representation of the hand in areas 3b and 1 in adult owl and squirrel monkeys.Neuroscience10, 639–665. [PubMed: 6646426]

Merzenich MM, Nelson RJ, Kaas JH, Stryker MP, Jenkins WM, et al., 1987. Variability in hand surface representations in areas 3b and 1 in adult owl and squirrel monkeys.J. Comparative Neurol258, 281–296.

Murata Y, Higo N, Oishi T, Yamashita A, Matsuda K, et al., 2008. Effects of motor training on the recovery of manual dexterity after primary motor cortex lesion in macaque monkeys.J. Neurophysiol99, 773–786. [PubMed: 18094104]

Nishimura Y, Morichika Y, Isa T, 2009. A subcortical oscillatory network contributes to recovery of hand dexterity after spinal cord injury.Brain132, 709–721. [PubMed: 19155271]

Nishimura Y, Onoe H, Morichika Y, Perfiliev S, Tsukada H, Isa T, 2007. Time-dependent central compensatory mechanisms of finger dexterity after spinal cord injury.Science (New York, N Y)318, 1150–1155.

Nout YS, Ferguson AR, Strand SC, Moseanko R, Hawbecker S, et al., 2012a. Methods for functional assessment after C7 spinal cord hemisection in the rhesus monkey.Neurorehabil. Neural Repair26, 556–569. [PubMed: 22331214]

Nout YS, Rosenzweig ES, Brock JH, Strand SC, Moseanko R, et al., 2012b. Animal models of neurologic disorders: a nonhuman primate model of spinal cord injury.Neurotherapeutics9, 380–392. [PubMed: 22427157]

Nudo RJ, 2013. Recovery after brain injury: mechanisms and principles.Front. Hum. Neurosci7, 887. [PubMed: 24399951]

Nudo RJ, Milliken GW, Jenkins WM, Merzenich MM, 1996a. Use-dependent alterations of movement representations in primary motor cortex of adult squirrel monkeys.J. Neurosci16, 785–807. [PubMed: 8551360]

Nudo RJ, Wise BM, SiFuentes F, Milliken GW, 1996b. Neural substrates for the effects of rehabilitative training on motor recovery after ischemic infarct.Science (New York, N Y)272, 1791–1794.

Pons TP, Wall JT, Garraghty PE, Cusick CG, Kaas JH, 1987. Consistent features of the representation of the hand in area 3b of macaque monkeys.Somatosens Res4, 309–331. [PubMed: 3589287]

Qi H-X, Reed JL, Franca JG, Jain N, Kajikawa Y, Kaas JH, 2016b. Chronic recordings reveal tactile stimuli can suppress spontaneous activity of neurons in somatosensory cortex of awake and anesthetized primates.J. Neurophysiol115, 2105–2123. [PubMed: 26912593]

Qi HX, Chen LM, Kaas JH, 2011. Reorganization of somatosensory cortical areas 3b and 1 after unilateral section of dorsal columns of the spinal cord in squirrel monkeys.J. Neurosci31, 13662–13675. [PubMed: 21940457]

Qi HX, Gharbawie OA, Wynne KW, Kaas JH, 2013. Impairment and recovery of hand use after unilateral section of the dorsal columns of the spinal cord in squirrel monkeys.Behav. Brain Res252, 363–376. [PubMed: 23747607]

Qi HX, Kaas JH, 2006. Organization of primary afferent projections to the gracile nucleus of the dorsal column system of primates.J. Comp. Neurol499, 183–217. [PubMed: 16977626]

Qi HX, Liao CC, Reed JL, Kaas JH, 2019. Reorganization of higher-order somatosensory cortex after sensory loss from hand in squirrel monkeys.Cereb. Cortex29, 4347–4365. [PubMed: 30590401]

Qi HX, Reed JL, Gharbawie OA, Burish MJ, Kaas JH, 2014. Cortical neuron response properties are related to lesion extent and behavioral recovery after sensory loss from spinal cord injury in monkeys.J. Neurosci34, 4345–4363. [PubMed: 24647955]

Qi HX, Wang F, Liao CC, Friedman RM, Tang C, et al., 2016a. Spatiotemporal trajectories of reactivation of somatosensory cortex by direct and secondary pathways after dorsal column lesions in squirrel monkeys.Neuroimage142, 431–453. [PubMed: 27523450]

Reed JL, Pouget P, Qi HX, Zhou Z, Bernard MR, et al., 2008. Widespread spatial integration in primary somatosensory cortex.Proc. Natl. Acad. Sci. USA105, 10233–10237. [PubMed: 18632579]

Rosenzweig ES, Courtine G, Jindrich DL, Brock JH, Ferguson AR, et al., 2010. Extensive spontaneous plasticity of corticospinal projections after primate spinal cord injury.Nat. Neurosci13, 1505–1510. [PubMed: 21076427]

Sasaki S, Isa T, Pettersson L-G, Alstermark B, Naito K, et al., 2004. Dexterous finger movements in primate without monosynaptic corticomotoneuronal excitation.J. Neurophysiol92, 3142–3147. [PubMed: 15175371]

Schmidlin E, Kaeser M, Gindrat A-D, Savidan J, Chatagny P, et al., 2011. Behavioral assessment of manual dexterity in non-human primates.J. Vis. Exp

Schmidlin E, Wannier T, Bloch J, Rouiller EM, 2004. Progressive plastic changes in the hand representation of the primary motor cortex parallel incomplete recovery from a unilateral section of the corticospinal tract at cervical level in monkeys.Brain Res1017, 172–183. [PubMed: 15261113]

Smirnakis SM, Schmid MC, Weber B, Tolias AS, Augath M, Logothetis NK, 2007. Spatial specificity of BOLD versus cerebral blood volume fMRI for mapping cortical organization.J. Cereb. Blood Flow Metab27, 1248–1261. [PubMed: 17213863]

Sofroniew MV, 2018. Dissecting spinal cord regeneration.Nature557, 343–350. [PubMed: 29769671]

Starkey ML, Schwab ME, 2012. Anti-Nogo-A and training: can one plus one equal three?Exp. Neurol235, 53–61. [PubMed: 21530508]

Sugiyama Y, Higo N, Yoshino-Saito K, Murata Y, Nishimura Y, et al., 2013. Effects of early versus late rehabilitative training on manual dexterity after corticospinal tract lesion in macaque monkeys.Journal of neurophysiology109, 2853–2865. [PubMed: 23515793]

Sur M, Nelson RJ, Kaas JH, 1982. Representations of the body surface in cortical areas 3b and 1 of squirrel monkeys: comparisons with other primates.J. Comp. Neurol211, 177–192. [PubMed: 7174889]

Taub E, 2014. Foreword for neuroplasticity and neurorehabilitation.Front. Hum. Neurosci8, 544. [PubMed: 25104931]

Taub E, Uswatte G, Elbert T, 2002. New treatments in neurorehabilitation founded on basic research.Nat Rev Neurosci3, 228–236. [PubMed: 11994754]

Taub E, Uswatte G, Mark VW, 2014. The functional significance of cortical reorganization and the parallel development of CI therapy.Front. Hum. Neurosci8, 396. [PubMed: 25018720]

Tetzlaff W, Fouad K, Kwon B, 2009. Be careful what you train for.Nat. Neurosci12, 1077–1079. [PubMed: 19710644]

Vanduffel W, Fize D, Mandeville JB, Nelissen K, Van Hecke P, et al., 2001. Visual motion processing investigated using contrast agent-enhanced fMRI in awake behaving monkeys.Neuron32, 565–577. [PubMed: 11719199]

Wahl AS, Omlor W, Rubio JC, Chen JL, Zheng H, et al., 2014. Neuronal repair. Asynchronous therapy restores motor control by rewiring of the rat corticospinal tract after stroke.Science (New York, N Y)344, 1250–1255.

Wall JT, Felleman DJ, Kaas JH, 1983. Recovery of normal topography in the somatosensory cortex of monkeys after nerve crush and regeneration.Science221, 771–773. [PubMed: 6879175]

Wong-Riley M, 1979. Changes in the visual system of monocularly sutured or enucleated cats demonstrable with cytochrome oxidase histochemistry.Brain Res171, 11–28. [PubMed: 223730]

Wu R, Su L, Yang P-F, Min Chen L, 2016. Altered spatiotemporal dynamics of cortical activation to tactile stimuli in somatosensory area 3b and area 1 of monkeys after spinal cord injury.eNeuro3.

Wu R, Yang P-F, Chen LM, 2017. Correlated disruption of resting-state fMRI, LFP, and spike connectivity between area 3b and s2 following spinal cord injury in monkeys.J. Neurosci37, 11192–11203. [PubMed: 29038239]

Xerri C, Coq JO, Merzenich MM, Jenkins WM, 1996. Experience-induced plasticity of cutaneous maps in the primary somatosensory cortex of adult monkeys and rats.J. Physiol. Paris90, 277–287. [PubMed: 9116682]

Yang PF, Qi HX, Kaas JH, Chen LM, 2014. Parallel functional reorganizations of somatosensory areas 3b and 1 and s2 following spinal cord injury in squirrel monkeys.J. Neurosci34 (28), 9351–9363 2014. [PubMed: 25009268]

Zaaimi B, Edgley SA, Soteropoulos DS, Baker SN, 2012. Changes in descending motor pathway connectivity after corticospinal tract lesion in macaque monkey.Brain135, 2277–2289. [PubMed: 22581799]

Zhang N, Wang F, Turner GH, Gore JC, Avison MJ, Chen LM, 2010. Intra- and inter-subject variability of high field fMRI digit maps in somatosensory area 3b of new world monkeys.Neuroscience165, 252–264. [PubMed: 19799969]

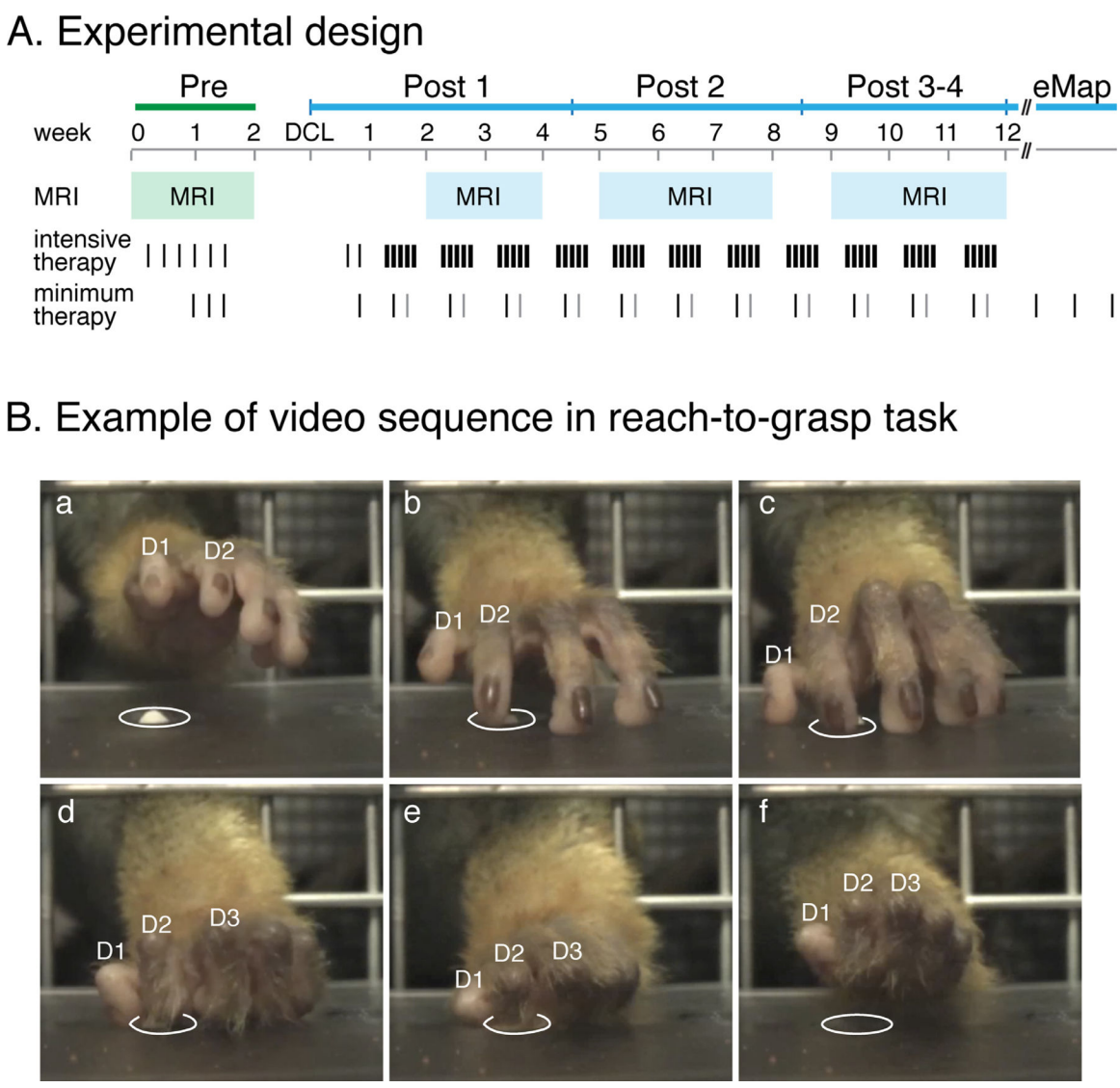


**Fig. 1.**

**A**. Experimental design. Schematic of the timelines for fMRI, behavioral training and testing. Thicker bars in "training" represent training session with higher number of retrievals (average 200 retrievals per training day), five days per week post-lesion; thin bars represent testing with less pellet retrievals (80 retrievals on average per testing day), 1 – 2 testing per week. B. Sequence of video clips of a typical post-lesion trial from squirrel monkey SM-Ur. **a – b**. monkey aims to pellet with digit 2; **c – d**. contacted the food pellet inside of wells with digit 2; **e – f**. retrieved the pellet inside of wells with digit 2 and secured it against the palm. The thumb was typically flexed throughout the grasp to secure the pellet against palm during retrieval. Thus, grasping in the present task was achieved with a power grip.

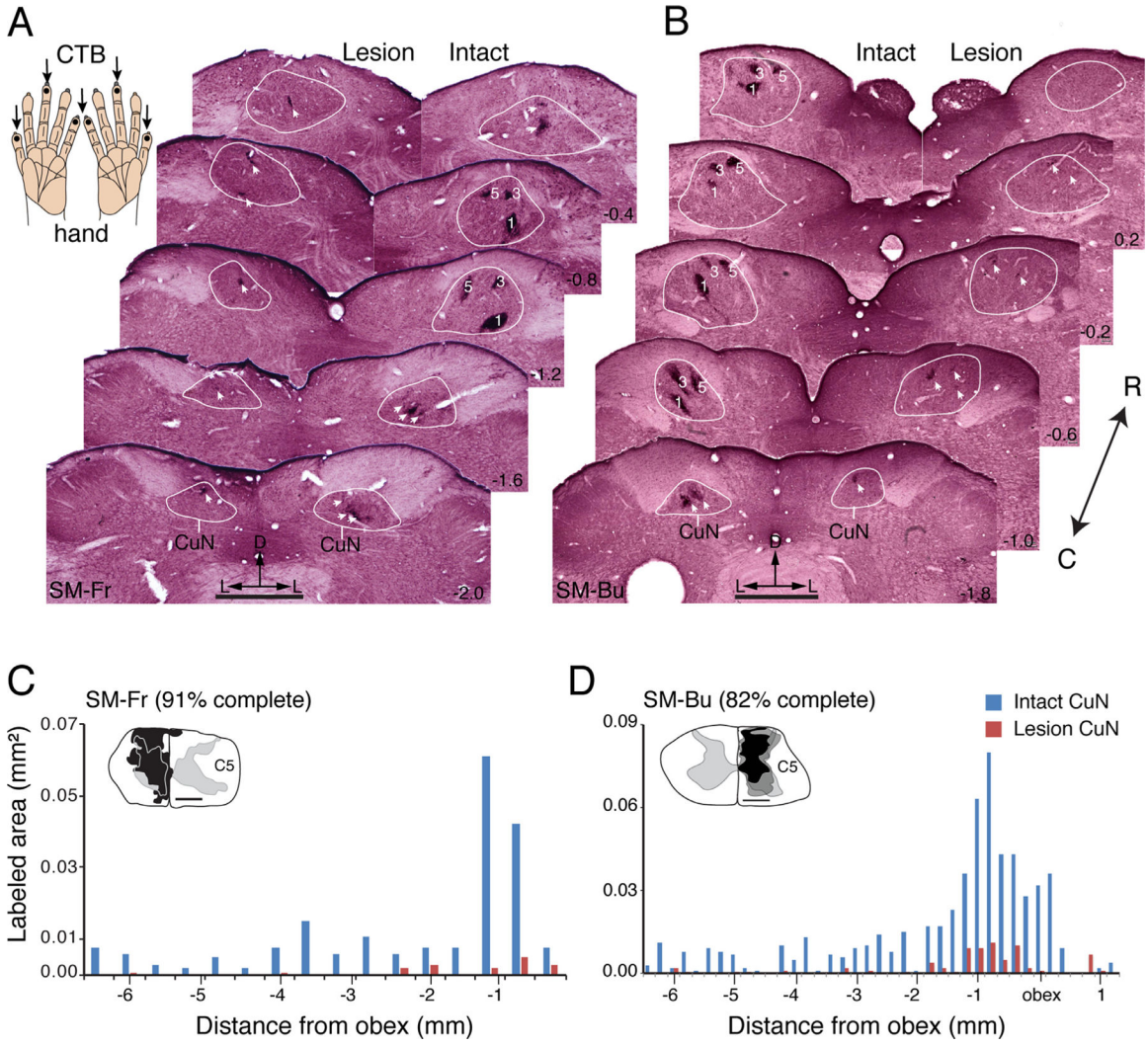


**Fig. 2.**

Example of effectiveness of the dorsal column lesion in squirrel monkey SM-Fr and SM-Bu. The dorsal column lesion was evaluated by comparing the amounts of labeled peripheral nerve terminations in the cuneate nucleus of the lesioned right side with the intact left side. **A and B**. Series of coronally cut cholera toxin subunit B (CTB) immunoreacted sections (labeled with numbers in italic on right) through dorsal column nuclei of brainstem in monkeys SM-Fr and SM-Bu. The cuneate nucleus is outlined in gray, and numbers 1, 3, 5 mark foci of afferents labeled by injections in digits 1, 3, and 5. Note that there are only a few detectable foci of axon fibers on the lesioned side where indicated by white arrows. The numbers on the right are series section numbers. **C and D**. Bar graphs compare the areal sizes of CTB-labeled axon arbor foci in the cuneate nuclei of the brainstem for the lesioned and intact sides for SM-Fr and SM-Bu. The numbers on the x-axis are the distance (in mm) measured from the beginning of the obex. The negative values indicate the measured distances were caudal to the obex. The y-axis value is the areal size (in $mm^2$) of the combined foci of CTB-label for each section through the cuneate nucleus of the brainstem. Insets on the top-left corner inside bar graphs are drawings of the reconstructed

transverse view of spinal cord through dorsal column lesions. Abbreviations, C4-C8, spinal cord cervical segments 4–8; CuN, cuneate nucleus of brainstem; C, caudal; D, dorsal; D1, D3, D5, digits 1, 3, 5; GN, gracile nucleus of brainstem; L, lateral; M, medial; R, rostral.

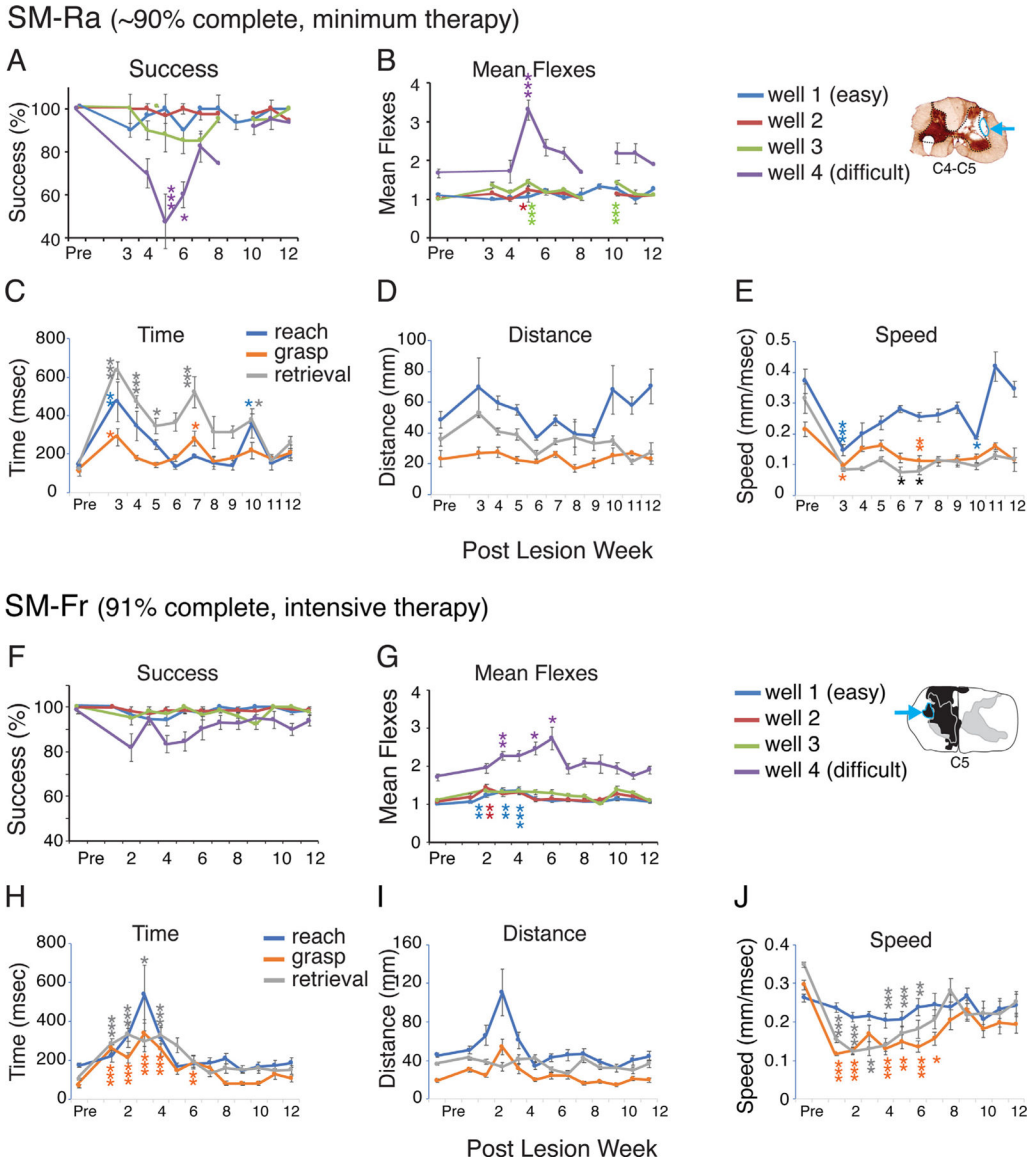


**Fig. 3.**

Evaluation of the impairment of hand use in reach-to-grasp task after unilateral dorsal column lesion (DCL) for two monkeys (SM-Ra and SM-Fr) with similar extent of DC-lesions. Percent of success and mean flexes (mean ± SEM) obtained from 4 testing wells of increasing depth/difficulties, in which the well 1 is the easiest, and well 4 is the most difficult. Mean kinematic measurements obtained from 5 successful trials from well 1. The Time, Distance, and Speed of monkeys' hands moved through space during the reach, grasp, and retrieval sequences. The insets in the right column are transverse views of spinal cord through DC-lesions, indicating the extent of the lesion. Note that DC-lesions encroached into a small portion of cortical spinal tract indicated by blue circles and blue arrows in monkeys SM-Ra and SM-Fr. Kruskal-Wallis Test (Nonparametric ANOVA) followed by Dunn's Multiple Comparisons was used to compare success score and kinematic trajectory

of hand use in the reach-to-grasp task before and after DCL of each monkey. Significance levels are indicated by ∗, $p < 0.05$; ∗∗ $p < 0.01$; ∗∗∗ $p < 0.001$.

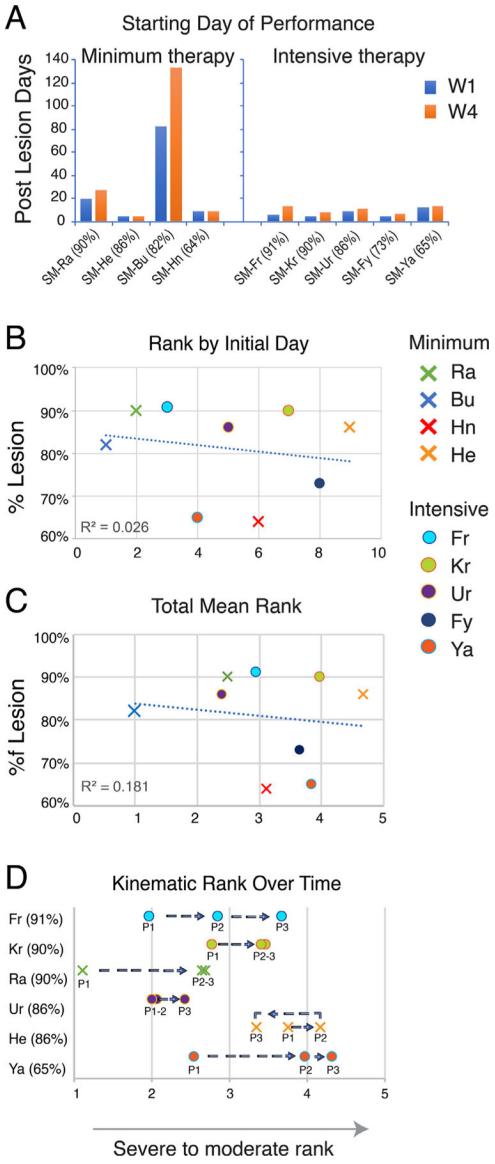


**Fig. 4.**

Relationship between severity of dorsal column lesion and behavioral outcome. **A**. Number of post-lesion days in which monkey was unable to grasp pellets from easy task (well 1, blue bars) or difficult task (well 4, orange bars) with the impaired hands. **B**. Relationship between extent of lesion and number of post-lesion days that monkey started to be able to perform the task, in which the more days of delaying task performance, the more behavioral impaired. **C**. Relationship between extent of lesion and total mean ranking of nine monkeys. The averaged ranking value (averaged up to 12 weeks post-lesion) was calculated from 11 measurements, they are mean differences between post- and pre-lesion values in percent of success, total digit flexes, time, distance, and speed during reach, grasp, and retrieval segments. Note that the rank value for two monkeys (SM-Bu and SM-Hn) was assigned based on the number of starting day of performance due to their lack of interest in sugar pellets. **D**. Behavioral recoveries of skill hand use in relation to lesion extent and post-lesion

experience. Monkeys are ranked on the percent completeness of the dorsal column lesion (65%–91%) and by kinematic rank value of hand use performance (1 – 5). Kinematic rank value are indicated by filled circles for monkeys with intensive behavioral therapy and by Xs for monkeys with minimum therapy (see text). Sequential testing periods are numbered with post-lesion weeks of P1 (1–4), P2 (5–8), and P3 (9–12).Numbers in x-axis represent ranking from most impaired (0) to least impaired (5 or 10). $R^2$ is the coefficient of determination from linear regression trendline. Dots are ranks from intensive behavioral therapy monkeys, crosses are from minimum behavioral therapy monkeys.

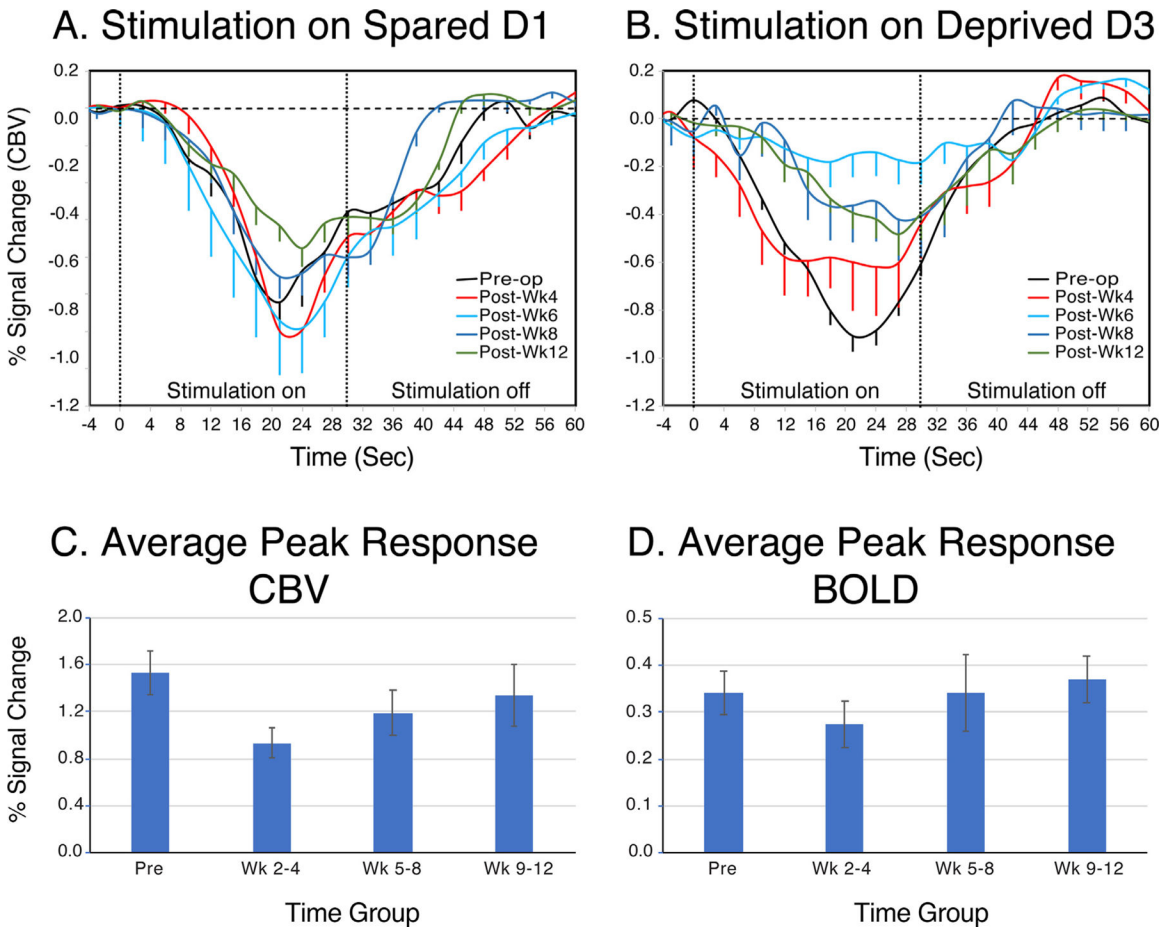


**Fig. 5.**

Examples of cerebral blood volume (CBV) signal time courses from significantly activated voxels in area 3b in response to vibrotactile stimulation on digits 1 and 3 before and four times after DC-lesion in squirrel monkey SM-Ya (65% complete). **A**. CBV response profiles to vibrotactile stimulation on spared digit 1 at pre-lesion and 4, 6, 8, and 12 weeks post-lesion. **B**. CBV response profiles to vibrotactile stimulation on mostly deprived D3 at pre-lesion and 4, 6, 8, and 12 weeks post-lesion. Dotted lines indicate the 30 sec duration of vibrotactile stimulation. The error bars show the standard deviation across voxels and epochs. **C.** and **D**. Pre- and post- op mean peak magnitudes of fMRI percent signal change (weighted-average) from significantly activated voxels in area 3b to vibrotactile stimulation on all digits of three CBV scanned monkeys (C) and six BOLD scanned monkeys (D). Although the overall magnitudes were different between CBV (rectified) and BOLD, they follow the same trend, in which the peak responses were initially declined at post-lesion weeks 2 – 4, and peak responses gradually recovered after post-lesion weeks 5 – 8.

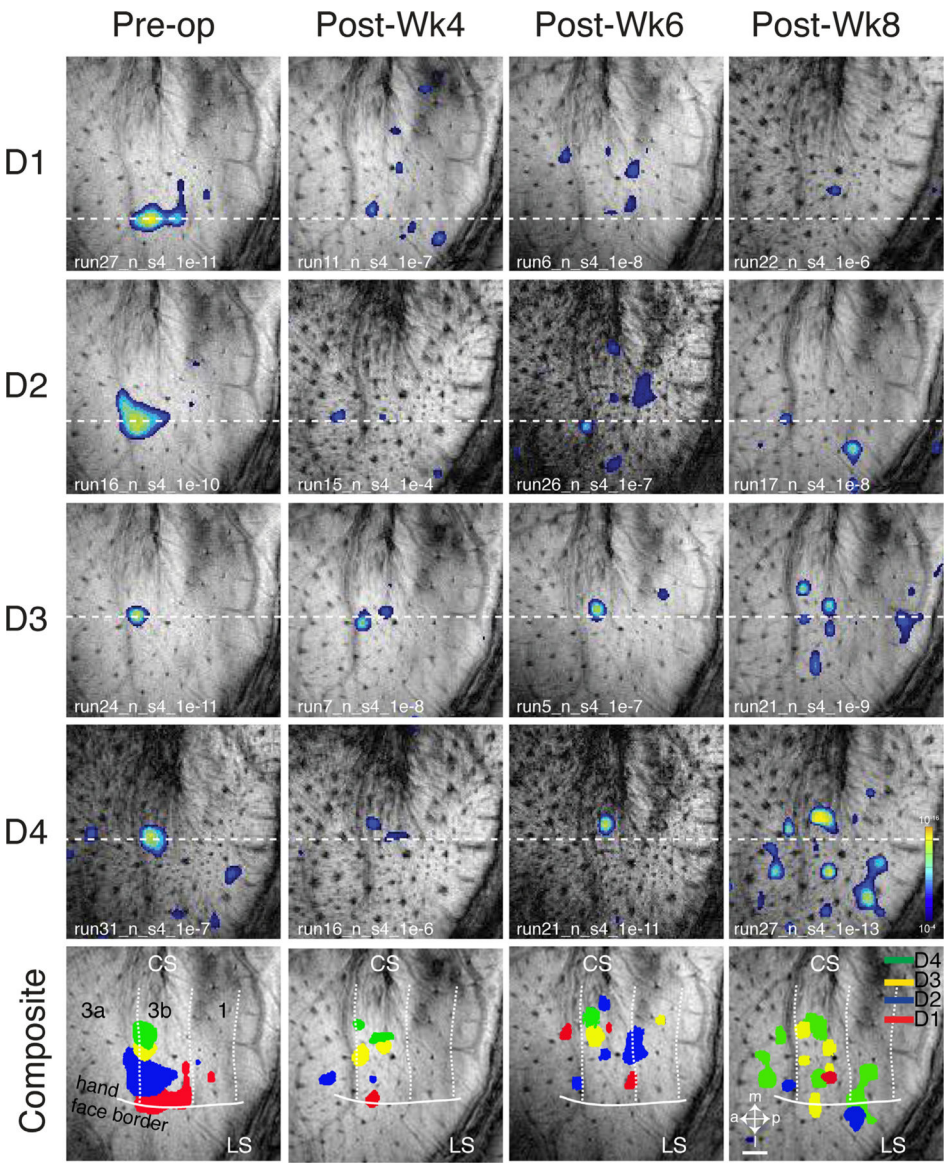


**Fig. 6.**

High-resolution CBV functional mapping of digit responses to vibrotactile stimulation for squirrel monkey SM-Bu. CBV functional images in somatosensory areas were collected with monocrystalline iron oxide nanoparticles (MION) enhancement in a 9.4 T scanner during stimulation of digits 1 – 4 at pre- and post-lesion weeks 4, 6, and 8. The white horizontal dashed lines throughout pre- and post-lesion images serve as comparative guidelines to help track mediolateral locations of fMRI activations in response to vibrotactile stimulation on the same digit throughout pre- and post-lesion scans; these lines are mediolaterally centered on the main focus of pre-lesion fMRI responses. Composite fMRI activation maps of digits 1 – 4 were obtained at pre- and post-lesion weeks. Dotted lines indicate the borders of areas 3b and 1. The strength of the evoked CBV responses is indicated from dark (weak) to light color (strong, see spectrum scale bar). The solid line indicates anatomically and electrophysiologically defined hand-face border with the face

lateral and the hand medial. The small white labels at the bottom of each panel indicate the scan sequence (run) number in an experiment, the adapted significant threshold value starting at $p < 10^{-4}$ or stronger (uncorrected for multiple comparisons). The panels without label indicate no significant ($p < 10^{-4}$) fMRI response was detected for that digit in the experiment. Abbreviations: 3a, 3b, 1, areas 3a, 3b, 1; a, anterior; CS, central sulcus; D1 – D5, digits 1 to 5; l, lateral; LS, lateral sulcus; m, medial; p, posterior. Scale = 1 mm.

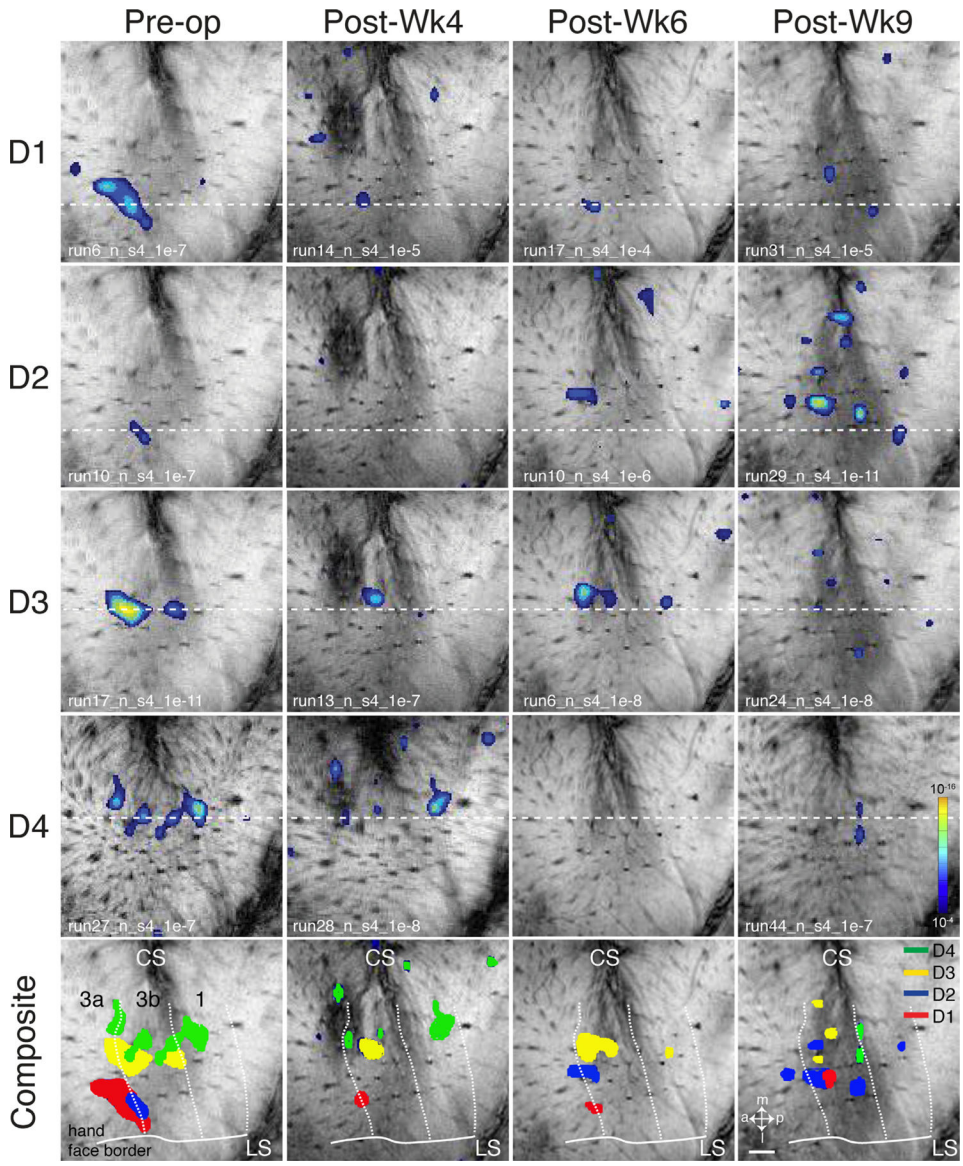


**Fig. 7.**

High-resolution CBV functional mapping of digit responses to vibrotactile stimulation for squirrel monkey SM-Fy. CBV functional images in somatosensory areas were collected with MION enhancement in a 9.4 T scanner during stimulation of digits 1 – 4 at pre- and post-lesion weeks 4, 6, and 9. The white horizontal dashed lines throughout pre- and post-lesion images serve as comparative guidelines to help track mediolateral locations of fMRI activations in response to vibrotactile stimulation on the same digit throughout pre- and post-lesion scans; these lines are mediolaterally centered on the main focus of pre-lesion fMRI responses. Composite fMRI activation maps of digits 1 – 4 were obtained at pre- and post-lesion weeks. Dotted lines indicate the borders of areas 3b and 1. The strength of the evoked CBV responses is indicated from dark (weak) to light color (strong, see spectrum scale bar). The small white labels at the bottom of each panel indicate the scan sequence (run) number in an experiment, the adapted significant threshold value starting at *p*

$< 10^{-4}$ or stronger (uncorrected for multiple comparisons). The panels without label indicate no significant ($p < 10^{-4}$) fMRI response was detected for that digit in the experiment. Conventions follow Fig. 6. Scale bar = 1 mm.

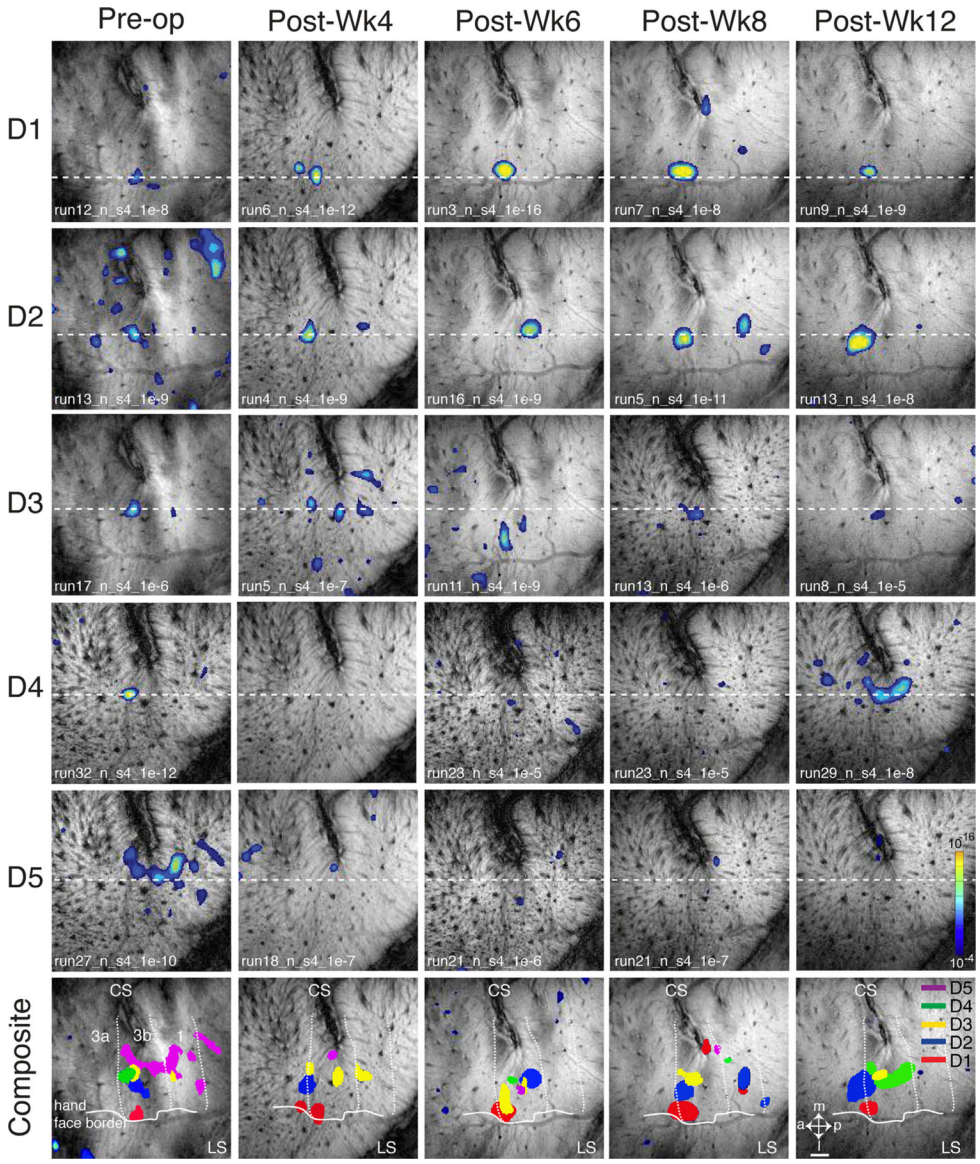


**Fig. 8.**

High-resolution CBV functional mapping of digit responses to vibrotactile stimulation for squirrel monkey SM-Ya. CBV functional images in somatosensory areas were collected with MION enhancement in a 9.4 T scanner during stimulation of digits 1 – 5 at pre- and post-lesion weeks 4, 6, 8 and 12. The white horizontal dashed lines throughout pre- and post-lesion images serve as comparative guidelines to help track mediolateral locations of fMRI activations in response to vibrotactile stimulation on the same digit throughout pre- and post-lesion scans; these lines are mediolaterally centered on the main focus of pre-lesion fMRI responses. Composite fMRI activation maps of all digits were obtained at pre- and post-lesion weeks. Dotted lines indicate the borders of areas 3b and 1. The strength of the evoked CBV responses is indicated from dark (weak) to light color (strong, see spectrum scale bar). The solid line indicates anatomically and electrophysiologically defined hand-face border with the face lateral and the hand medial. The small white labels

at the bottom of each panel indicate the scan sequence (run) number in an experiment, the adapted significant threshold value starting at $p < 10^{-4}$ or stronger (uncorrected for multiple comparisons). The panels without label indicate no significant ($p < 10^{-4}$) fMRI response was detected for that digit in the experiment. Conventions follow Fig. 6. Scale bar = 1 mm. Part of series panels (Panels of “D1” and “D4” series) have been shown in previous published book chapter, Chapter 4.25 “Cortical and Subcortical Plasticity After Sensory Loss in the Somatosensory System of Primates”, The Sense, A comprehensive Reference, second edition, Edited by Bernd Fritzsch, Academic Press 2020.

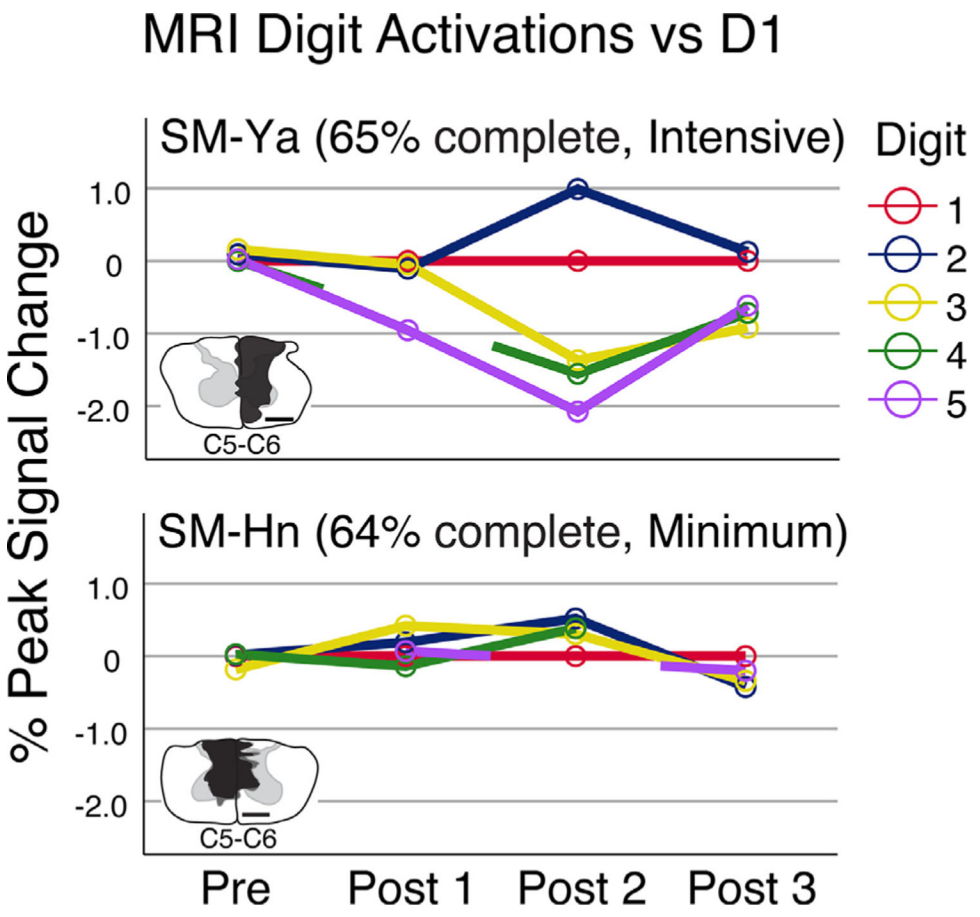


**Fig. 9.**

Differences in percent signal change in response to D1 stimulation compared to stimulation of other digits within a scan session indicating consistency or variability. Open circles, lines are color-coded to indicate digit stimulation condition. Missing circles, broken lines indicate that a digit was not stimulated during the missing scan time period. SM-Ya, with a lesion at a lower cervical level that partly spared axons representing D1 and D2.The responses of D3-D5 were lower in percent signal change compared to the D1 response, while D2 stimulation activated larger peak signal change at the second post-lesion scan. D1 and D2 returned to similar proportions, and D3-D5 were only slightly less by post-lesion scan 3. The insets in the lower-left corner are transverse views of spinal cord through DC-lesions, indicating the extent of the lesion.

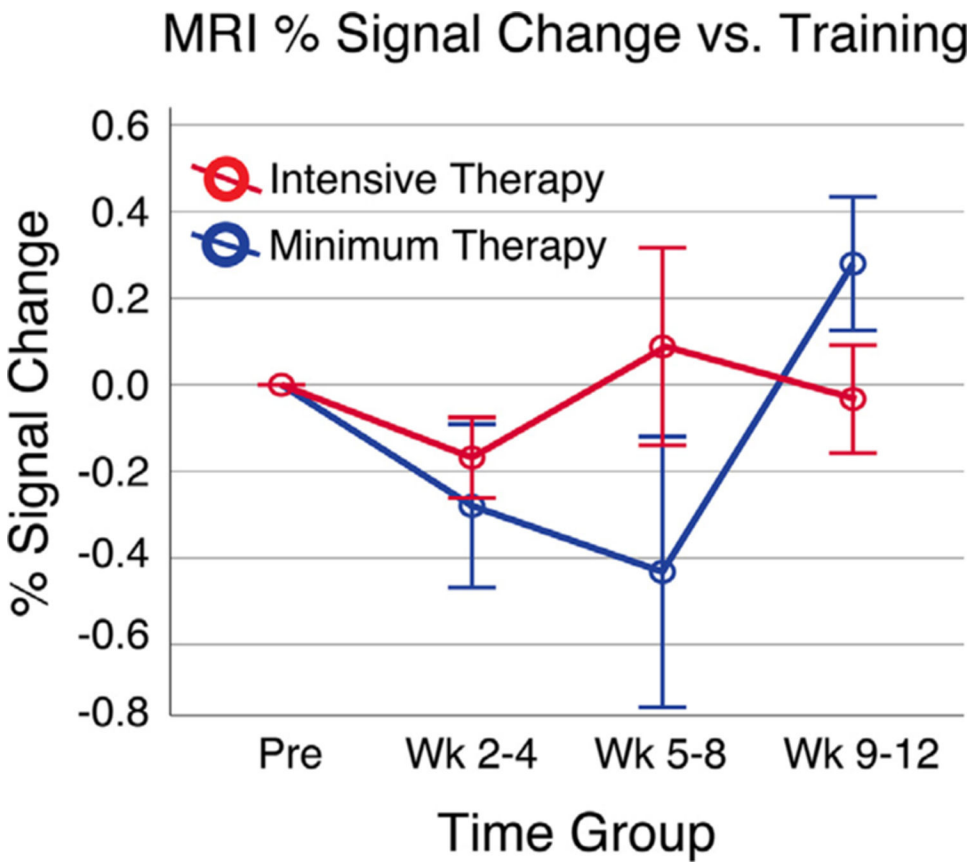


**Fig. 10.**

Relationship between strengths of fMRI response and the extent of lesion. Rectified differences from pre-lesion show a tendency from intensive behavioral therapy to improve responses to nearly normal level between 5 – 8 post-lesion weeks.

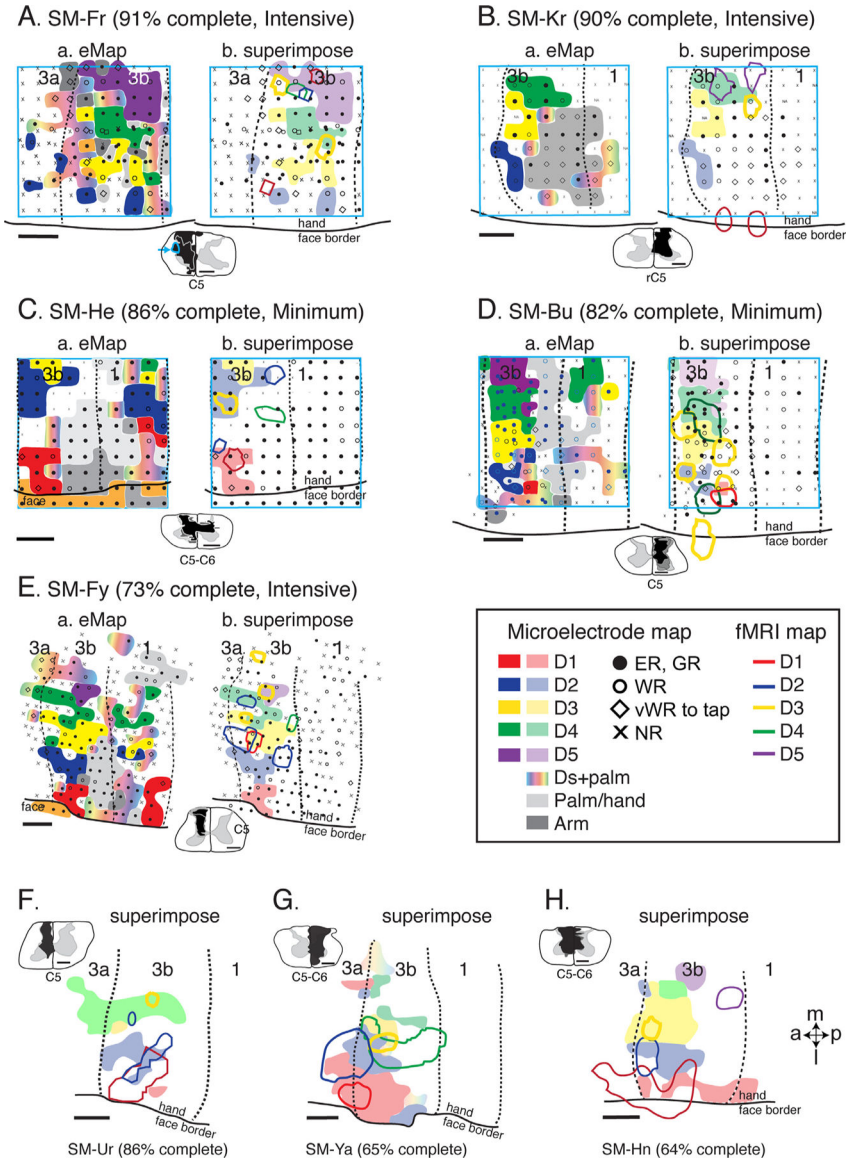


**Fig. 11.**

Co-registrations of fMRI maps with the electrophysiological maps for eight monkeys. **A – D**: Somatotopic maps of areas 3b and 1 were obtained with 100-electrode arrays recordings (marked with blue boxes). The maps were reconstructed based on the locations of receptive fields for neurons at each electrode. **E**: Somatotopic map of areas 3b and 1 was obtained with single microelectrode mapping. For extensive electrophysiological mapping results for squirrel monkeys SM-Ur (**F**), SM-Ya (**G**), and SM-Hn (**H**), see Liao et al. (2016). fMRI maps are in color-coded outlines, and electrophysiological maps are in the same color-coded solid shades. Solid dots mark responses ranging from good to excellent at a given mapping site; open circles mark weak responses; open diamonds mark very weak response to hard taps; x's mark microelectrode penetrations with no responses; '-' marks disabled electrodes. Dotted lines indicate the rostral and caudal borders of area 3b, and solid lines mark hand-face border in area 3b defined by topography and anatomical architecture. The insets near

electrophysiological maps are transverse views of spinal cord through DC-lesions, indicating the extent of the lesion. Abbreviations: 3a, 3b, and 1, somatosensory areas 3a, 3b and 1; a, anterior; D1 – D5, digits 1 to 5; Ds, multiple digits; ER, excellent response; GR, good response; l, lateral; m, medial; NR, no response; p, posterior; R, rostral; vWR, very weak response; WR, weak response; Scale bars = 1 mm.

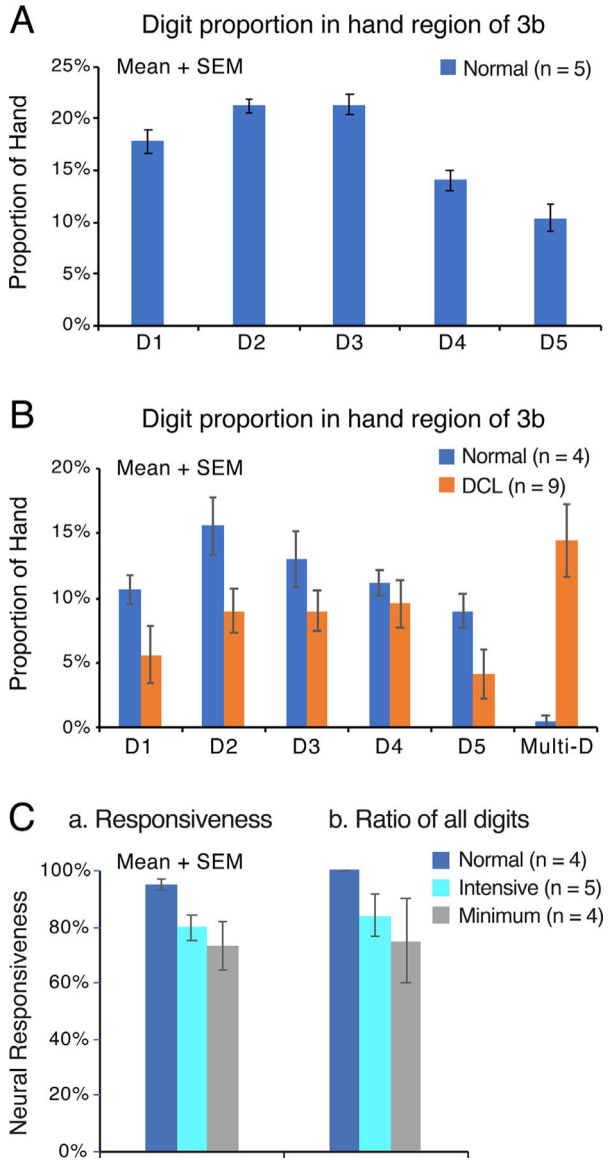


**Fig. 12.**

**A**. Bar graph shows the size of each digit representation as a proportion of the whole hand representation from Merzenich et al. (1987). Tabulated results of 5 normal squirrel monkeys. The graph depicts that digits 2 and 3 representations were the largest, followed by digits 1, 4, and 5. **B**. Bar graph shows the size of each digit representation as a proportion of the whole hand representation from 4 normal monkeys (blue bars) and 9 DC-lesion monkeys with or without intensive behavioral therapy (orange bars). **Ca**. Percent of neuronal responsiveness in the hand region of area 3b in 4 normal monkeys (blue bar), 5 intensive behavioral therapy monkeys (sky blue bar) and 4 minimum behavioral therapy monkeys (gray bar) indicate the effects of DC-lesion and trends of training effect. **Cb**, percent of all five digits in normal monkeys (blue bar), 5 intensive behavioral therapy monkeys (sky blue bar) and 4 minimum behavioral therapy monkeys (gray bar) in the hand region of area 3b. The graph shows that

all five digits were not always represented in lesioned monkeys. In normal monkeys, all 5 digits are represented (100%).

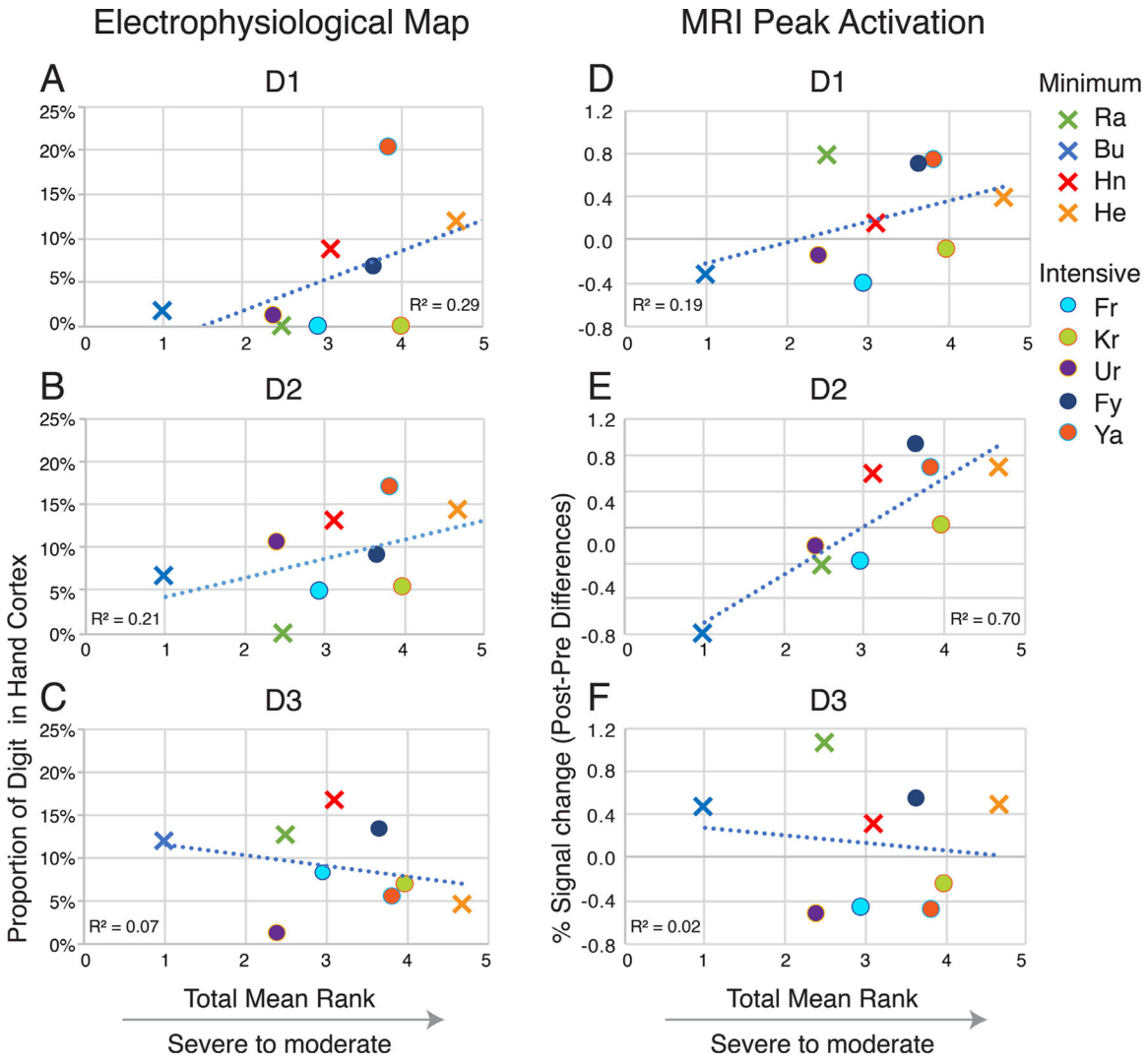


**Fig. 13.**

Relationship between reactivated digit responses in area 3b and total mean ranking of nine lesioned monkeys. **A – C**. Relationship between the proportion of digits 1 – 3 territories in total hand region of area 3b obtained from microelectrode mapping and the total mean ranking of nine monkeys. **D – F**. Relationship between magnitudes of the peak signal change of the fMRI responses to vibrotactile stimulation on digits 1 – 3 and total mean ranking. Averaged ranking value was calculated from mean differences between post- and pre-lesion values (averaged up to 12 weeks post-lesion) in total digit flexes, percent of success, time, distance, and speed during reach, grasp, and retrieval segments. Numbers in x-axis represent ranking from most impaired (0) to least impaired (5). $R^2$ is the coefficient of determination from linear regression trendline. Dots represent intensive behavioral therapy monkeys, crosses represent minimum behavioral therapy monkeys. The color-coded symbols for each monkey are consistent with those of Fig. 4.

**Table 1**

Case information.

| Group | Cases | Lesion level | Lesion extent | Recovery time (days/weeks) | Types of fMRI and scan time (week) | Train/test |
|---|---|---|---|---|---|---|
| **Extensive** | SM-Fr | C5 | 91% | 491/70 | BOLD (pre-, post-wk 2, 5, 8) | Intensive therapy |
| | SM-Kr | rC5 | 90% | 184/26 | BOLD (pre-, post-wk 4, 9) | Intensive therapy |
| | SM-Ra | border of C4-C5 | >90% | 169/25 | BOLD (pre-, post-wk 3, 8, 16) | Minimum therapy |
| **Intermediate** | SM-He | border of C5-C6 | 86% | 129/18 | BOLD (pre-, post-wk 4, 10) | Minimum therapy |
| | SM-Ur | C5 | 86% | 414/59 | BOLD (pre-, post-wk 4, 6, 8, 12) | Intensive therapy |
| | SM-Bu | C5 | 82% | 133/19 | CBV (pre-, post-wk 4, 6, 8) | Minimum therapy |
| | SM-Fy | C5 | 73% | 100/14 | CBV (pre-, post-wk 4, 6, 9) | Intensive therapy |
| **Less extensive** | SM-Ya | border of C5-C6 | 65% | 292/42 | CBV (pre-, post-wk 4, 6, 8, 12) | Intensive therapy |
| | SM-Hn | border of C5-C6 | 64% | 142/20 | BOLD (pre-, post-wk 2, 5, 8) | Minimum therapy |